15. Pietschmann T, Kaul A, Koutsoudakis G, Shavinskaya A, Kallis S, Steinmann E, et al. Construction and characterization of infectious intragenotypic and intergenotypic hepatitis C virus chimeras. Proc Natl Acad Sci U S A 2006;103:7408-7413.
16. Kato T, Date T, Murayama A, Morikawa K, Akazawa D, Wakita T. Cell culture and infection system for hepatitis C virus. Nat Protoc 2006;1:2334-2339.
17. Wakita T. Isolation of JFH-1 strain and development of an HCV infection system. Methods Mol Biol 2009;510:305-327.
18. Wakita T, Pietschmann T, Kato T, Date T, Miyamoto M, Zhao Z, et al. Production of infectious hepatitis C virus in tissue culture from a cloned viral genome. Nat Med 2005;11:791-796.
19. Saeed M, Suzuki R, Kondo M, Aizaki H, Kato T, Mizuochi T, et al. Evaluation of hepatitis C virus core antigen assays in detecting recombinant viral antigens of various genotypes. J Clin Microbiol 2009;47:4141-4143.
20. Takeuchi T, Katsume A, Tanaka T, Abe A, Inoue K, Tsukiyama-Kohara K, et al. Real-time detection system for quantification of hepatitis C virus genome. Gastroenterology 1999;116:636-642.
21. Date T, Miyamoto M, Kato T, Morikawa K, Murayama A, Akazawa D, et al. An infectious and selectable full-length replicon system with hepatitis C virus JFH-1 strain. Hepatol Res 2007;37:433-443.
22. Kato T, Date T, Miyamoto M, Furusaka A, Tokushige K, Mizokami M, et al. Efficient replication of the genotype 2a hepatitis C virus subgenomic replicon. Gastroenterology 2003;125:1808-1817.
23. Date T, Kato T, Kato J, Takahashi H, Morikawa K, Akazawa D, et al. Novel cell culture-adapted genotype 2a hepatitis C virus infectious clone. J Virol 2012;86:10805-10820.
24. Zhong J, Gastaminza P, Cheng G, Kapadia S, Kato T, Burton DR, et al. Robust hepatitis C virus infection in vitro. Proc Natl Acad Sci U S A 2005;102:9294-9299.
25. Olmstead AD, Knecht W, Lazarov I, Dixit SB, Jean F. Human subtilase SKI-1/S1P is a master regulator of the HCV Lifecycle and a potential host cell target for developing indirect-acting antiviral agents. PLoS Pathog 2012;8:e1002468.
26. Kato T, Matsumura T, Heller T, Saito S, Sapp RK, Murthy K, et al. Production of infectious hepatitis C virus of various genotypes in cell cultures. J Virol 2007;81:4405-4411.
27. Miyanari Y, Atsuzawa K, Usuda N, Watashi K, Hishiki T, Zayas M, et al. The lipid droplet is an important organelle for hepatitis C virus production. Nat Cell Biol 2007;9:1089-1097.
28. Gastaminza P, Dryden KA, Boyd B, Wood MR, Law M, Yeager M, et al. Ultrastructural and biophysical characterization of hepatitis C virus particles produced in cell culture. J Virol 2010;84:10999-11009.
29. Zhong J, Gastaminza P, Chung J, Stamataki Z, Isogawa M, Cheng G, et al. Persistent hepatitis C virus infection in vitro: coevolution of virus and host. J Virol 2006;80:11082-11093.
30. Anderson N, Borlak J. Molecular mechanisms and therapeutic targets in steatosis and steatohepatitis. Pharmacol Rev 2008;60:311-357.
31. Gavrilova O, Haluzik M, Matsusue K, Cutson JJ, Johnson L, Dietz KR, et al. Liver peroxisome proliferator-activated receptor gamma contributes to hepatic steatosis, triglyceride clearance, and regulation of body fat mass. J Biol Chem 2003;278:34268-34276.
32. Videla LA, Rodrigo R, Orellana M, Fernandez V, Tapia G, Quinones L, et al. Oxidative stress-related parameters in the liver of non-alcoholic fatty liver disease patients. Clin Sci (Lond) 2004;106:261-268.
33. Ma S, Yang D, Li D, Tan Y, Tang B, Yang Y. Inhibition of uncoupling protein 2 with genipin exacerbates palmitate-induced hepatic steatosis. Lipids Health Dis 2012;11:154.
34. Perlemuter G, Sabile A, Letteron P, Vona G, Topilco A, Chretien Y, et al. Hepatitis C virus core protein inhibits microsomal triglyceride transfer protein activity and very low density lipoprotein secretion: a model of viral-related steatosis. FASEB J 2002;16:185-194.
35. Mirandola S, Realdon S, Iqbal J, Gerotto M, Dal Pero F, Bortoletto G, et al. Liver microsomal triglyceride transfer protein is involved in hepatitis C liver steatosis. Gastroenterology 2006;130:1661-1669.
36. Jackel-Cram C, Babiuk LA, Liu Q. Up-regulation of fatty acid synthase promoter by hepatitis C virus core protein: genotype-3a core has a stronger effect than genotype-1b core. J Hepatol 2007;46:999-1008.

## Supporting Information

Additional Supporting Information may be found in the online version of this article at the publisher's website.

AQ1: Author: Please verify names and affiliations of all authors. Also, check contact information for correspondence (address, email, fax).

OPEN ACCESS Freely available online

PLOS ONE

# Involvement of MAP3K8 and miR-17-5p in Poor Virologic Response to Interferon-Based Combination Therapy for Chronic Hepatitis C

**Akihito Tsubota[1,2]*, Kaoru Mogushi[3], Hideki Aizaki[4], Ken Miyaguchi[3], Keisuke Nagatsuma[1,2], Hiroshi Matsudaira[1,2], Tatsuya Kushida[5], Tomomi Furihata[6], Hiroshi Tanaka[3], Tomokazu Matsuura[7]**

**1** Institute of Clinical Medicine and Research (ICMR), Jikei University School of Medicine, Kashiwa, Chiba, Japan, **2** Division of Gastroenterology and Hepatology, Kashiwa Hospital, The Jikei University School of Medicine, Kashiwa, Chiba, Japan, **3** Department of Bioinformatics, Medical Research Institute, Tokyo Medical and Dental University, Bunkyo-ku, Tokyo, Japan, **4** Department of Virology II, National Institute of Infectious Diseases, Shinjuku-ku, Tokyo, Japan, **5** National Bioscience Database Center, Japan Science and Technology Agency, Chiyoda-ku, Tokyo, Japan, **6** Laboratory of Pharmacology and Toxicology, Graduate School of Pharmaceutical Science, Chiba University, Chiba, Japan, **7** Department of Laboratory Medicine, Jikei University School of Medicine, Minato-ku, Tokyo, Japan

## Abstract

Despite advances in chronic hepatitis C treatment, a proportion of patients respond poorly to treatment. This study aimed to explore hepatic mRNA and microRNA signatures involved in hepatitis C treatment resistance. Global hepatic mRNA and microRNA expression profiles were compared using microarray data between treatment responses. Quantitative real-time polymerase chain reaction validated the gene signatures from 130 patients who were infected with hepatitis C virus genotype 1b and treated with pegylated interferon-alpha and ribavirin combination therapy. The correlation between mRNA and microRNA was evaluated using *in silico* analysis and *in vitro* siRNA and microRNA inhibition/overexpression experiments. Multivariate regression analysis identified that the independent variables IL28B SNP rs8099917, hsa-miR-122-5p, hsa-miR-17-5p, and MAP3K8 were significantly associated with a poor virologic response. MAP3K8 and miR-17-5p expression were inversely correlated with treatment response. Furthermore, miR-17-5p repressed HCV production by targeting MAP3K8. Collectively, the data suggest that several molecules and the inverse correlation between mRNA and microRNA contributed to a host genetic refractory hepatitis C treatment response.

**Citation:** Tsubota A, Mogushi K, Aizaki H, Miyaguchi K, Nagatsuma K, et al. (2014) Involvement of MAP3K8 and miR-17-5p in Poor Virologic Response to Interferon-Based Combination Therapy for Chronic Hepatitis C. PLoS ONE 9(5): e97078. doi:10.1371/journal.pone.0097078

**Editor:** Wenyu Lin, Harvard Medical School, United States of America

**Received** December 6, 2013; **Accepted** April 14, 2014; **Published** May 12, 2014



**Funding:** This work was supported in part by Grants-in-Aid from the Ministry of Health, Labour and Welfare (Japan), the Ministry of Education, Culture, Sports, Science and Technology (Japan), and Clinical Research Funds from ICMR, the Jikei University School of Medicine. The funders had no role in study design, data collection and analysis, decision to publish, or preparation of the manuscript.

**Competing Interests:** The authors have declared that no competing interests exist.

* E-mail: atsubo@jikei.ac.jp

## Introduction

Chronic hepatitis C (CH-C) caused by hepatitis C virus (HCV) infection is a major chronic liver disease worldwide, and it often develops into cirrhosis and hepatocellular carcinoma. Pegylated interferon alpha (peg-IFNα) and ribavirin (RBV) combination therapy is widely used to treat CH-C [1]. However, treatment fails in approximately 50% patients with HCV genotype 1. Of note, approximately 20–30% patients show null or partial response to the treatment. The introduction of nonstructural 3/4A protease inhibitors has improved the outcome for genotype 1 CH-C patients [1]. However, new antiviral agents increase the frequency and severity of adverse effects, are costly, have complex treatment regimens, and often result in viral resistance. Importantly, the outcomes of triple combination therapy are extremely poor in patients who showed null and partial response to previous peg-IFNα/RBV, compared to treatment-naïve patients and relapsers [1–3]. Furthermore, over 50% of null and partial responders, among all patients with a similar virologic response or viral kinetics, relapse after treatment cessation [2,3]. Collectively, these studies suggest a role of host genetics in treatment resistance.

Microarray applications in clinical medicine identified that numerous mRNAs and microRNAs (miRNAs) regulate complex processes involved in disease development. For example, hepatic mRNA expression of IFN-stimulated genes (ISGs, such as ISG15, OAS, IFI, IP10, and viperin) and IFN-related pathway genes (MX and USP18) correlate with responses to peg-IFNα/RBV combination therapy for CH-C [4–7]. However, few studies have examined global miRNAs alone [8]. Furthermore, mRNA and miRNA gene signatures and their interactions in treatment response have not been reported. miRNAs are evolutionarily conserved, small non-coding RNAs [9,10]. A single miRNA can regulate the expression of multiple target mRNAs and their encoded proteins by imperfect base pairing and subsequent mRNA cleavage/translational repression. Conversely, the expression of a single mRNA is often regulated by several miRNAs. As regulators of promotion or suppression of gene expression, miRNAs are involved in diverse biological and physiological processes, including cell cycle, proliferation, differentiation, and apoptosis. In addition to targeting endogenous mRNAs, miRNAs regulate the life cycle of viruses such as the Epstein-Barr virus,

HCV, and other oncogenic viruses by interacting with viral transcripts [11,12].

We investigated the differential expression profiles of mRNAs and miRNAs isolated from the liver tissues of untreated patients with HCV genotype 1b using microarray analysis. Expression profiles and their interactions were analyzed to identify the molecular signatures associated with treatment resistance.

## Materials and Methods

### Patient population, treatment, and liver tissue samples

During 2010 and 2011, 130 patients infected with HCV genotype 1b were treated weekly with 1.5 μg/kg of peg-IFNα-2b (MSD, Tokyo) and daily with 600–1000 mg RBV (MSD) [2,3] for 48 weeks at Jikei University Kashiwa-affiliated hospitals. Patients with undetectable serum HCV RNA at week 12 or later were recommended to extend the treatment to 72 weeks. All study participants provided informed written consent and materials for genetic testing and met the following criteria: (1) CH-C diagnosis confirmed by laboratory tests, virology, and histology; (2) genotype 1b confirmed by polymerase chain reaction (PCR)-based method; (3) absence of malignancy, liver failure, or other form of chronic liver disease; and (4) no concurrent treatment with any other antiviral or immunomodulatory agent. Liver specimens were obtained percutaneously before treatment, formalin-fixed, and paraffin-embedded for histological assessment [13]. A tissue section was stored in RNA*later* solution (Life Technologies, Carlsbad, CA). Total RNA containing mRNA and miRNA was isolated using the mirVana miRNA isolation kit (Life Technologies).

Sustained virological response (SVR) was defined as an undetectable serum HCV RNA level at 24 weeks after treatment completion. A null response was defined as a viral decline of $< 2 \log_{10}$ IU/mL from baseline at treatment week 12 and detectable HCV RNA during treatment. A partial response was defined as a viral decline of $>2 \log_{10}$ IU/mL from baseline at week 12, with no achievement of an undetectable HCV RNA level. Relapse was defined as an undetectable serum HCV RNA level at the end of treatment and viremia reappearance on follow-up examination [1]. Viral loads and the presence or absence of serum HCV RNA were evaluated using a qualitative PCR assay (Amplicor HCV version 2.0; Roche Diagnostics, Tokyo).

This study conformed to the provisions of the Declaration of Helsinki and Good Clinical Practice guidelines and was approved by the Jikei University Ethics Committee for Human Genome/Gene Analysis Research (No.21-093_5671).

### mRNA microarray

Global mRNA expression analysis was performed using total RNA isolated from each sample [sustained virological responders (SVRs), $n=5$; relapsers, $n=3$; null responders, $n=4$] and the GeneChip Human Genome U133 Plus 2.0 Array (Affymetrix, Santa Clara, CA). Datasets were normalized by the robust multi-array analysis, using R 2.12.1 statistical software and the BioConductor package.

### miRNA microarray

Global miRNA expression analysis was performed using total RNA isolated from the same samples used for mRNA expression analysis and the miRCURY LNA microRNA Array series (Exiqon, Vedbaek, Denmark). Total RNA was labeled with Hy3 and hybridized to slides that contained capture probes targeting all human miRNAs registered in the miRBASE 14.0. miRNA microarray datasets were normalized by quantile normalization using R statistical software.

### Differential gene expression according to treatment response

The limma package from BioConductor software (under R statistical software) was used to calculate moderated t-statistics (based on the empirical Bayes approach) to identify mRNA or miRNA differentially expressed between the SVR/relapser group and null/partial responder group. Because of multiple hypothesis testing, $p$ values were adjusted by the Benjamini-Hochberg false discovery rate (FDR) method.

### Hierarchical cluster analysis

Up- and down-regulated probe sets were analyzed by hierarchical clustering using R statistical software. Pearson's correlation coefficients were used to calculate a matrix similarity score among the probe sets. The complete linkage method was used for agglomeration. Heat maps were generated from significant differentially expressed probe sets.

### Quantitative real-time PCR for mRNA

To validate microarray results and to confirm the observed differences in the mRNA expression levels in a quantitative manner, each sample was subjected to reverse transcription (RT)-PCR and quantitative real-time RT-PCR (qPCR) in triplicate. After cDNA synthesis, target genes were amplified in PCR mixtures that contained TaqMan Universal PCR Master Mix (Life Technologies) and TaqMan probes designed with the Universal Probe Library Assay Design Center (http://www.roche-applied-science.com/sis/rtpcr/upl/adc.jsp). Target gene expression levels in each sample were normalized to the expression of the housekeeping gene of 18S rRNA and the corresponding gene of one null responder.

### Quantitative real-time PCR for miRNA

cDNA was synthesized from aliquots of the isolated total RNA using the TaqMan MicroRNA Reverse Transcription kit (Life Technologies) including RT primers designed with miRNA-specific stem-loop structures according to manufacturer's protocol. miRNA expression levels were quantified with the TaqMan MicroRNA assay (Life Technologies) in triplicate. Target gene expression levels were normalized in each sample to the expression of the endogenous gene RNU48 and the corresponding gene of one null responder.

### miRNA target prediction

Up- and down-regulated miRNAs with a fold change of $>1.2$ and $p<0.005$ (FDR$<0.15$) between two groups (SVRs/relapsers *vs* null responders) in the microarray analysis were subjected to the *in silico* prediction of mRNA targets for miRNA using MicroCosm Targets, miRanda, PicTar, PITA, and TargetScan algorithms. Predicted mRNA targets were analyzed further if they met the following criteria: (1) fold change of $>1.5$ and $p<0.003$ (FDR$<$ 0.35) in mRNA microarray results; (2) inverse correlation (negative correlation coefficient) between miRNA and mRNA in mRNA and miRNA microarray results; and (3) qPCR-validated microarray results. Kyoto Encyclopedia of Genes and Genomes (KEGG) Pathways, Agilent Literature Search 3.0.3 beta, and Cytoscape 3.0.2 were used to identify the significance of candidates in gene regulatory networks.

### Cell culture

The human hepatoma cell line Huh7.5.1 (a gift from Professor Francis Chisari, Scripps Research Institute, La Jolla, CA) was maintained in Dulbecco's modified Eagle's medium containing 10% fetal bovine serum [14]. Cell culture-produced HCV (HCVcc) were harvested from JFH1-transfected Huh7.5.1 as previously described [15].

### Plasmids and siRNAs

The siRNAs targeting MAP3K8 were siRNA1, 5′-uucgucuuuauaucuugugtt-3′; siRNA2, 5′-uguugcuagguuuaauauctt-3′; siRNA3, 5′-aucuugugccaaguauacctt-3′; and scrambled negative control siRNA to siRNA1 (Sigma-Aldrich, St. Louis, MO). The expression and inhibitor plasmids of hsa-miR-17-5p and control plasmids were purchased from GeneCopoeia (Rockville, MD).

### HCV core antigen measurements and cell viability

The HCV core antigen concentrations in filtered culture medium and cell lysates of infected cells were measured with the Lumipulse Ortho HCV antigen kit (Ortho Clinical Diagnostics, Tokyo). Cell viability was analyzed using the CellTiter-Glo Luminescent Cell Viability Assay (Promega, Madison, WI).

### Transfection

Cells were seeded into a 24-well plate and transfected with siRNAs and plasmids using Lipofectamine RNAiMAX (Invitrogen, San Diego, CA) and TransIT-LT1 (Mirus, Madison, WI), respectively.

### Luciferase reporter assay

The MAP3K8 3′UTR segment containing the putative miR-17-5p target sites was subcloned into the pGL3 reporter plasmid (Promega). A mutant construct was also generated by PCR-based mutagenesis using mutagenic primers. The luciferase reporter and hsa-miR-17-5p expressing or mock plasmids were co-transfected with the *Renilla* luciferase transfection control plasmid. Luciferase reporter activity was measured 48 hours after transfection with the Dual-Luciferase Reporter Assay System (Promega).

### Western blot

Liver samples were sonicated in lysis buffer. Lysate aliquots were separated by SDS-polyacrylamide gel electrophoresis and transferred onto a nitrocellulose membrane. Membranes were incubated with primary antibodies against MAP3K8 (ab70853, Abcam, San Diego, CA) and β-actin (EP1123Y, Abcam). Membranes were incubated with horseradish peroxidase-conjugated secondary antibodies. Immunoreactivity was detected with reagents (GE Healthcare Life Sciences, Piscataway, NJ). Images were scanned and band intensities quantified with Image J.

### IL28B and ITPA single nucleotide polymorphism (SNP) genotyping

Genomic DNA was extracted from whole blood using the MagNA Pure LC and the DNA Isolation Kit (Roche Diagnostics). The IL28B rs8099917 and rs12979860 [16,17] and ITPA exon 2 rs1127354 [18] genetic polymorphisms were genotyped by real-time detection PCR with the TaqMan SNP Genotyping Assays.

### Statistical analysis for factors associated with null/partial response

The chi-square, Fisher's exact, Student's *t*, and the Mann–Whitney two-tailed tests were used to compare frequencies in categorical data or differences in continuous data between two groups. Significant independent factors associated with null/partial responses were identify with multiple logistic regression analysis using the SPSS statistical package for Windows, version 17.0 (IBM SPSS, Chicago, IL). A $p$ value of $<0.05$ was considered statistically significant.

## Results

### Patient profiles and treatment response

Among the 130 patients, 62 (48%) achieved SVR, 36 (28%) relapsed, and six (5%) and 26 (20%) showed partial and null response, respectively. Patients were divided into an SVR/relapser group and a null/partial responder group. Table S1 compares the baseline characteristics of the two groups. Patients with elevated serum gamma glutamyl transpeptidase and decreased albumin concentrations were more likely to experience a null/partial response. The IL28B rs8099917 TG and rs12979860 CT variants were more likely to be null/partial responders compared with TT and CC genotypes, respectively.

### mRNAs associated with treatment response

mRNA microarray data were deposited into the NCBI Gene Expression Omnibus (GEO) (http://www.ncbi.nlm.nih.gov/geo/), accession number GSE42697. The cut-off criteria for fold change $>1.5$ and $p<0.003$ identified 39 up-regulated and 17 down-regulated annotated probe sets in null responders (Data S1). The up-regulated genes were associated with transcription, translation, cell cycle, phosphorylation, signal transduction, immune response, RNA splicing/mRNA processing, and viral reproduction. The down-regulated genes were associated with xenobiotic/small molecule/lipid metabolic and oxidation–reduction processes. Hierarchical clustering of mRNAs and samples showed that samples from SVRs and relapsers clustered to form a group different from the null responders (Fig. S1). To validate the microarray results, qPCR was performed for all significant differentially expressed genes. The expression levels of MAP3K8 (mitogen-activated protein kinase kinase kinase 8, $p=5.24\times10^{-7}$), TMEM178 (transmembrane protein 178, $p=7.31\times10^{-6}$), PSME4 (proteasome activator subunit 4, also known as *PA200*, $p=2.43\times10^{-4}$), and EIF3B (eukaryotic translation initiation factor-3B, $p=3.16\times10^{-6}$; Fig. 1) were significantly increased in null/partial responders compared with those in SVRs/relapsers. TMEM178 is a multi-pass membrane protein and PSME4 is a nuclear protein that activates the proteasome and is important for oxidative-stress adaptation. EIF3B is involved in protein translation/synthesis and interacts with the HCV IRES and the 40S ribosomal subunit.

### miRNAs associated with treatment response

miRNA microarray data were deposited into the NCBI GEO, accession number GSE45179. The cut-off criteria for fold change $>1.2$ and $p<0.005$ identified 111 down-regulated and 76 up-regulated miRNAs in null responders (Data S2). Hierarchical two-dimensional clustering showed that distinct patient groups clustered into two distinct groups (Fig. S2). Bioinformatic analysis predicted target genes of the differentially expressed miRNAs. The hypothetical target genes should be MAP3K8, TMEM178, PSME4, and EIF3B. Furthermore, these miRNAs and mRNAs must have an inverse correlation between mRNA and miRNA microarray data. The microRNAs that satisfied the requirements were as follows: hsa-let-7g* and hsa-miR-17-5p, -20b, -297, -374b, -494, -602, -668, and -1297 for MAP3K8; hsa-miR-106b* and -122-5p for TMEM178; and hsa-miR-492 and -675-5p for PSME4. No corresponding miRNA was identified for EIF3B.

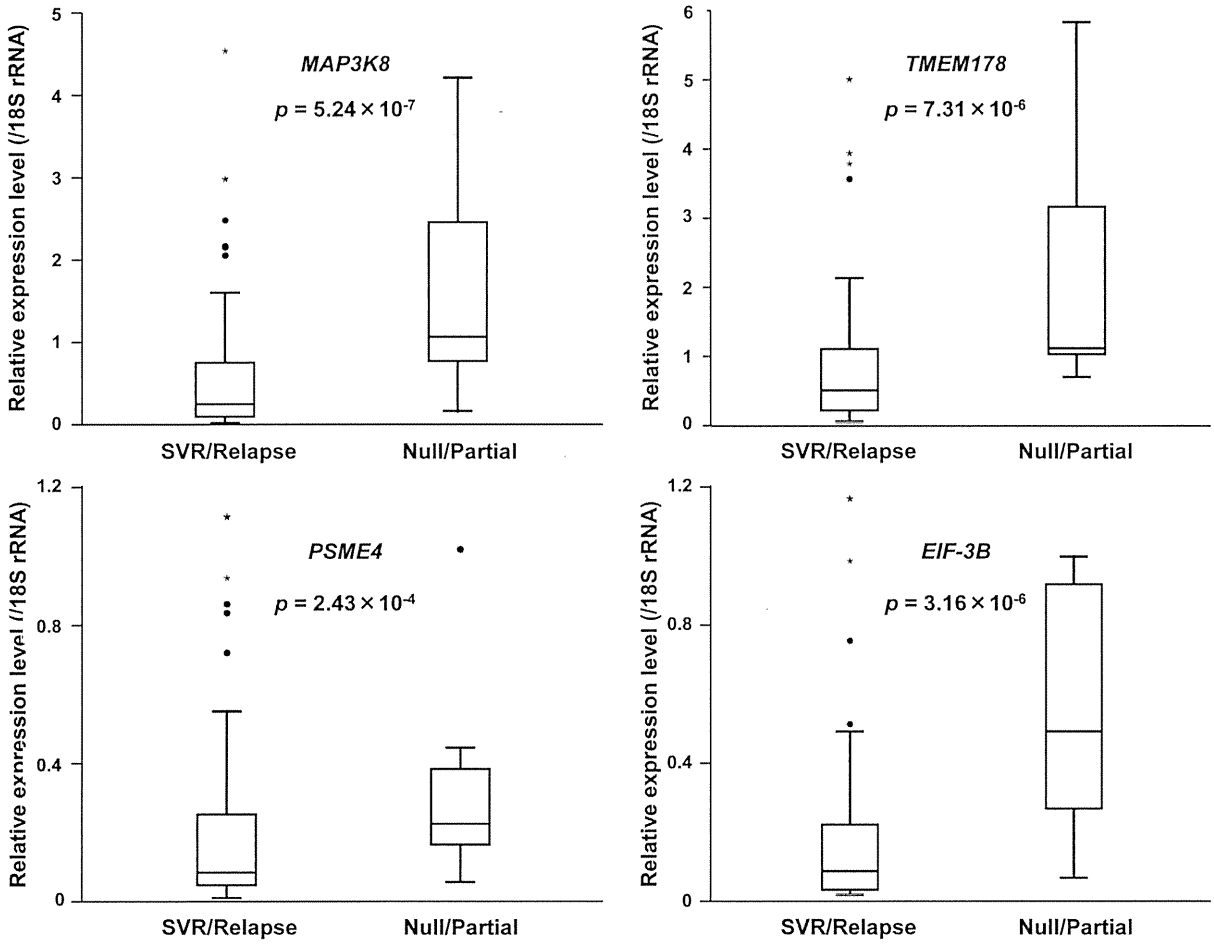


**Figure 1. Validation of differentially expressed mRNAs by qPCR analysis.** The expression levels of four mRNAs were significantly higher in null/partial responders than in SVRs/relapsers. Assays for each sample were performed in triplicate. All *p*-values were calculated using the Mann–Whitney test.
doi:10.1371/journal.pone.0097078.g001

Stem-loop-based qPCR was performed to confirm the reliability of the miRNA microarray results and the inverse correlation between miRNA and mRNA. The expression levels of hsa-miR-122-5p ($p = 2.75 \times 10^{-8}$), hsa-miR-675-5p ($p = 1.00 \times 10^{-5}$), and hsa-miR-17-5p ($p = 1.73 \times 10^{-8}$) were significantly lower in null/partial responders than in SVRs/relapsers (Fig. 2).

## Independent variables associated with treatment response

Multiple logistic regression analysis of variables that were significant in univariate analysis identified that rs8099917 [$p = 3.67 \times 10^{-3}$, odds ratio (OR) = 7.51, 95% confidence interval (CI) = 2.14–29.27], hsa-miR-122-5p ($p = 5.60 \times 10^{-4}$, OR = 0.11, 95% CI = 0.03–0.38), hsa-miR-17-5p ($p = 2.02 \times 10^{-4}$, OR = 0.56, 95% CI = 0.41–0.76), and MAP3K8 ($p = 8.58 \times 10^{-3}$, OR = 2.86, 95% CI = 1.31–6.25) were significantly associated with null/partial response. Importantly, *in silico* analysis and microarray data suggested that increased miR-17-5p could cause MAP3K8 reduction. In fact, an inverse correlation was observed between MAP3K8 mRNA and miR-17-5p ($r = -0.592$, $p = 4.31 \times 10^{-3}$). MAP3K8 is closely linked to genes associated with cell proliferation, inflammation, and apoptosis (Fig. S3) and is associated with the miR-17 cluster family (Fig. S4).

## MAP3K8 contributes to HCV production

siRNA transfection in HCVcc-infected cells was performed to assess the influence of MAP3K8 mRNA and protein on HCV production (Fig. 3A). miR-17-5p levels were significantly increased (Fig. 3B) while supernatant HCV core antigen levels were significantly decreased following transfection of the siRNAs (Fig. 3C). However, the HCV core antigen levels in cell lysates were not changed (Fig. 3C). Taken together, these findings suggested that MAP3K8 repressed miR-17-5p and contributed to the production (e.g. release and assembly) of HCV. *In vivo*, MAP3K8 protein expression levels were significantly increased in null/partial responders compared with those in SVRs/relapsers ($p = 2.43 \times 10^{-5}$).

## Hsa-miR-17-5p regulates HCV production by targeting MAP3K8

Changes in MAP3K8 and HCV core antigen levels were evaluated by hsa-miR-17-5p inhibition and overexpression in HCVcc-infected cells. miR-17-5p inhibition increased MAP3K8 mRNA and protein levels (Fig. 4A and 4B, left). In contrast, miR-17-5p overexpression decreased MAP3K8 mRNA and protein levels (Fig. 4A and 4B, right). Interestingly, miR-17-5p inhibition increased, whereas miR-17-5p overexpression decreased HCV core antigen levels in both supernatants and cell lysates (Fig. 4C).

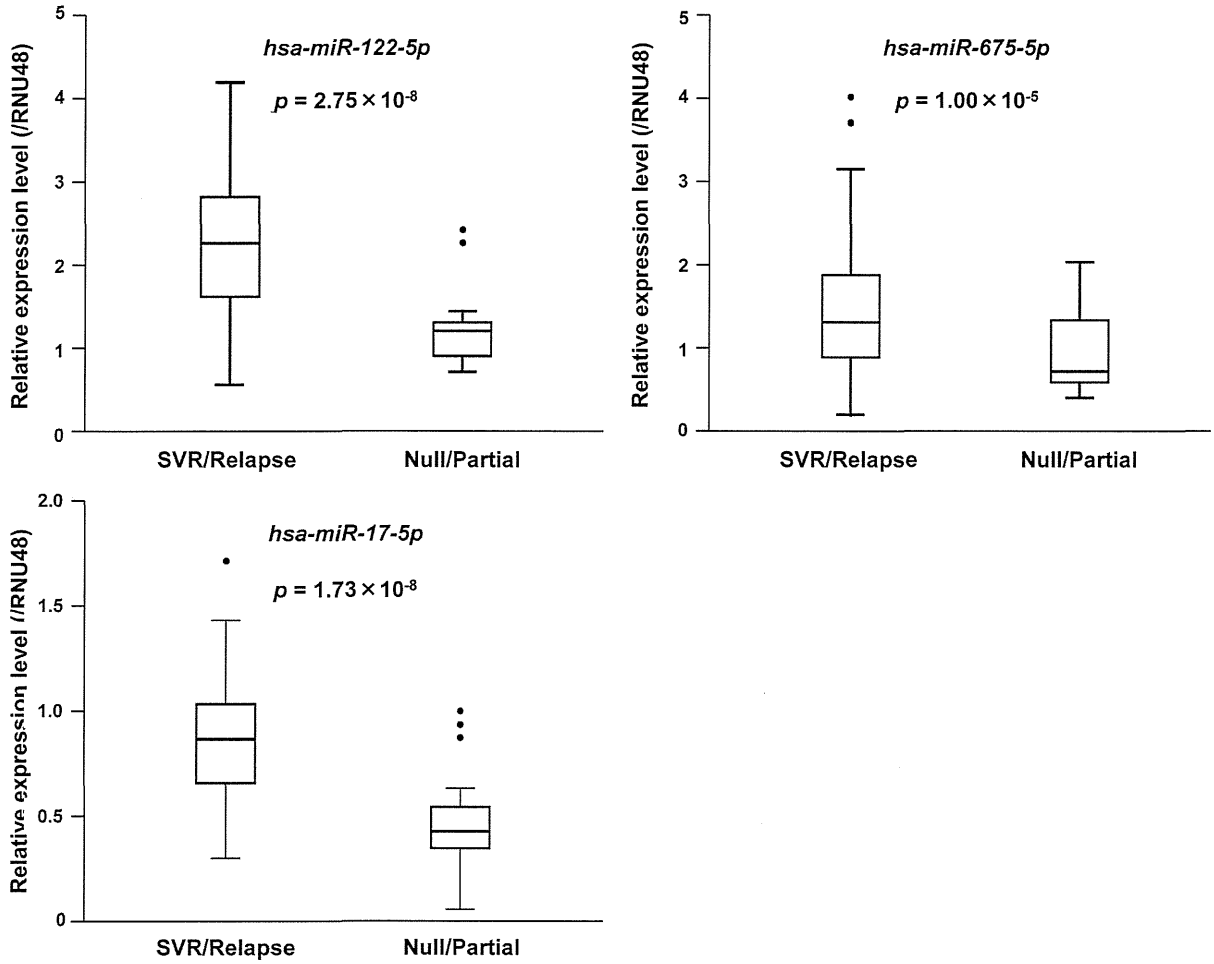


**Figure 2. Validation of differentially expressed miRNAs by qPCR analysis.** The expression levels of three miRNAs were significantly higher in null/partial responders than in SVRs/relapsers. Assays for each sample were performed in triplicate. All *p*-values were calculated using the Mann–Whitney test.
doi:10.1371/journal.pone.0097078.g002

Taken together, these results suggested that miR-17-5p regulated the production of HCV by targeting MAP3K8 mRNA. Luciferase reporter assays showed that miR-17-5p overexpression decreased the luciferase activity of the wild-type MAP3K8 3′UTR reporter construct, whereas co-transfection with the mutant MAP3K8 3′UTR construct or mock had no effect (Fig. 5), suggesting that miR-17-5p targeted the MAP3K8 3′UTR and antagonized MAP3K8 protein expression.

## Discussion

This study showed close linkage between mRNA and miRNA signatures in CH-C treatment outcomes using global expression profiling analyses. To confirm the findings, this cohort was randomly divided into derivation and confirmatory groups. The derivation group results were similar to those described above and reproducible in the confirmatory group (data not shown). Subsequently, we attempted to compare our findings with registered patient data obtained from independent cohorts comprising either Asian or non-Asian subjects. However, comparisons were not possible because most mRNA or miRNA microarray studies had a small sample size, limited information, unregistered data, and/or findings that were not validated in an independent cohort [4–7,11,19–21]. To our knowledge, our study was the first to investigate the correlation between mRNA and miRNA in treatment response using global gene expression analysis and *in vitro* experiments. Such gene signature identification can improve the accuracy of treatment outcome predictions, independent of known strong predictors.

Pretreatment hepatic ISG levels are higher in non-SVRs/non-relapsers than in SVRs/relapsers [4–7]. The poor ISG response of non-SVRs with further exogenous IFN may contribute to treatment failure [5,6]. Because patient groups with different response categories differ in their innate IFN response to HCV infection; poor responders may have adopted a different equilibrium in their innate immune response to HCV [4,6]. As per multivariate regression analysis, however, IL28B SNPs may diminish the significance of hepatic ISGs as treatment predictors because hepatic ISG expression is associated with IL28B SNPs [7,19]. Conversely, hepatic ISGs were reported to be stronger predictors compared with IL28B SNPs [20]. Although our gene set enrichment analysis (data not shown) also showed that hepatic ISG expression levels were generally higher in null/partial responders than in SVRs/relapsers, the differences were not large enough to be ranked in a higher order and/or to reach statistical significance in expression profiling and validation analyses (Data S3). These variations among studies may be caused by different and heterogeneous patient characteristics, including HCV geno-

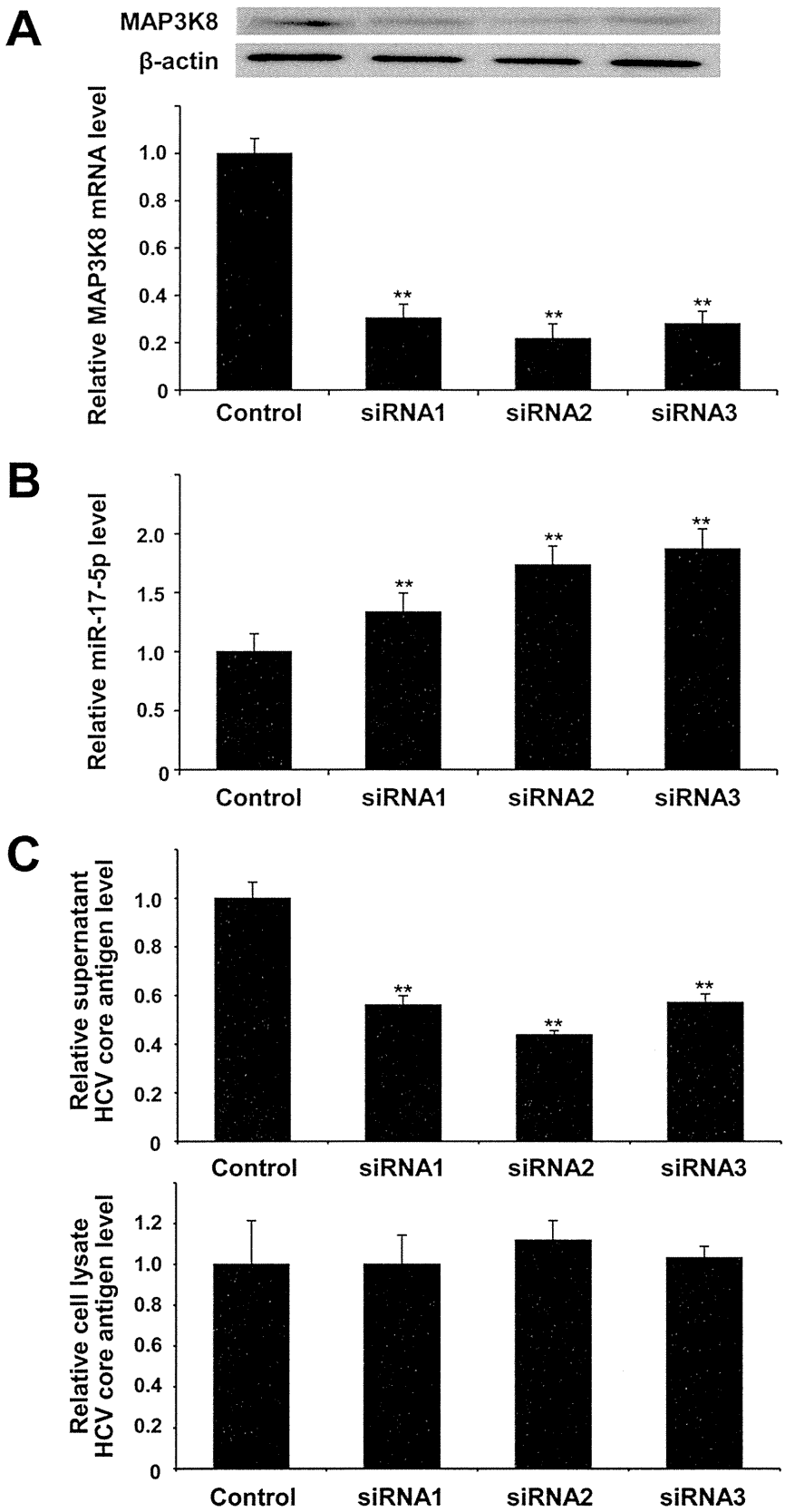


**Figure 3. Transfection of Huh7.5.1 cells with siRNAs against MAP3K8.** (**A**) Transfection of Huh7.5.1 cells with siRNAs against MAP3K8 significantly decreased intracellular MAP3K8 mRNA levels, (**B**) increased intracellular hsa-miR-17-5p levels, and (**C**) decreased HCV core antigen levels in the supernatant, and had no effect on those in cell lysate. Bars indicate the means of three independent experiments and the error bars indicate standard deviations. All *p*-values were calculated using two-tailed Student's *t*-test. $^{**}p<0.001$ compared with controls.
doi:10.1371/journal.pone.0097078.g003

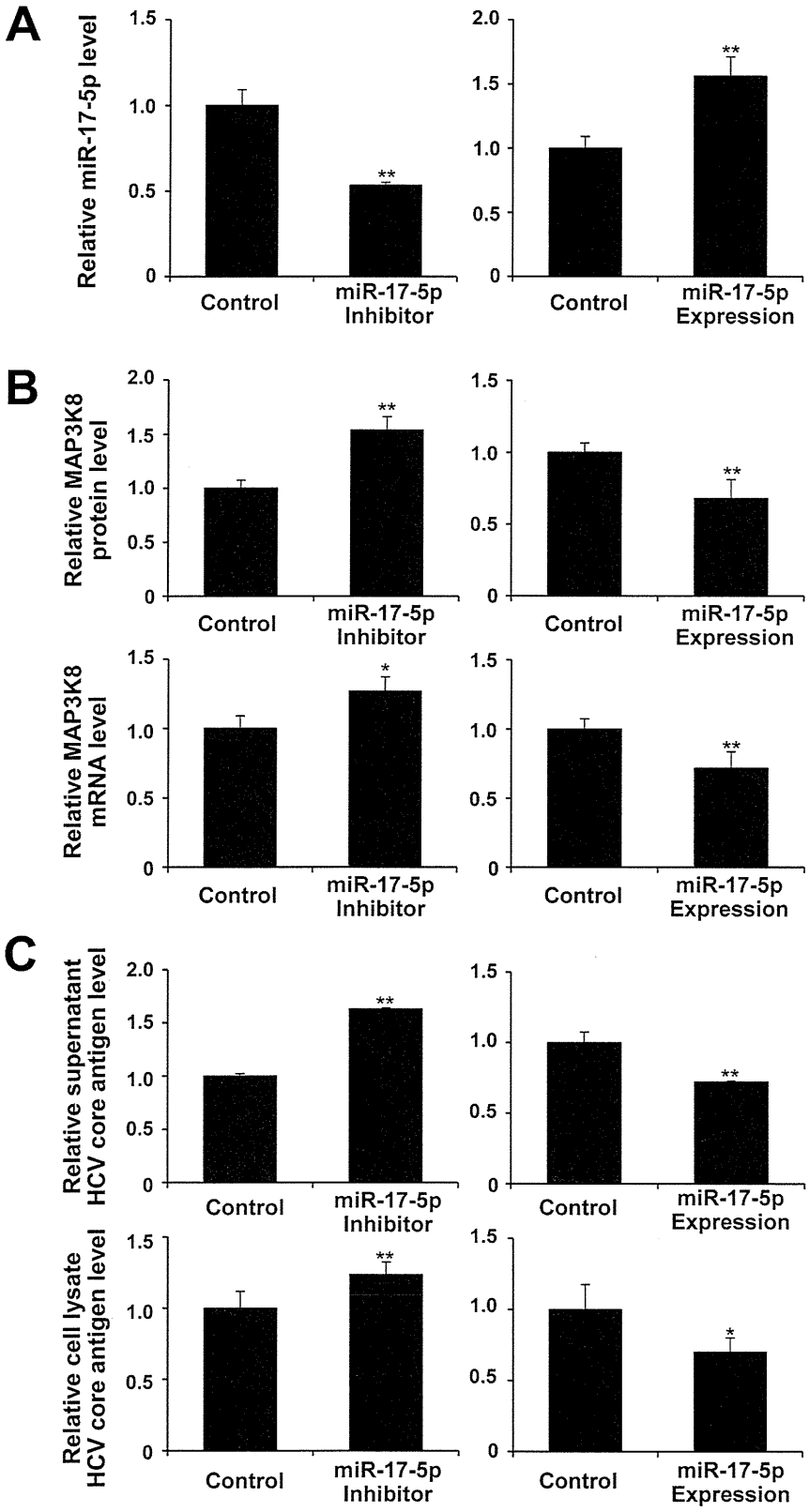


**Figure 4. Expression and inhibition of hsa-miR-17-5p in Huh7.5.1 cells.** (**A**) Functional suppression (left) and overexpression (right) plasmids of miR-17-5p. (**B**) Inhibition of miR-17-5p increased (left), whereas overexpression of miR-17-5p decreased MAP3K8 mRNA and protein expression levels (right). (**C**) HCV core antigen levels increased following miR-17-5p inhibition (left) and decreased by miR-17-5p overexpression (right) in both supernatant and cell lysate. Bars indicate the means of three independent experiments and the error bars indicate standard deviations. *$p<0.01$ and **$p<0.001$ compared with controls.
doi:10.1371/journal.pone.0097078.g004

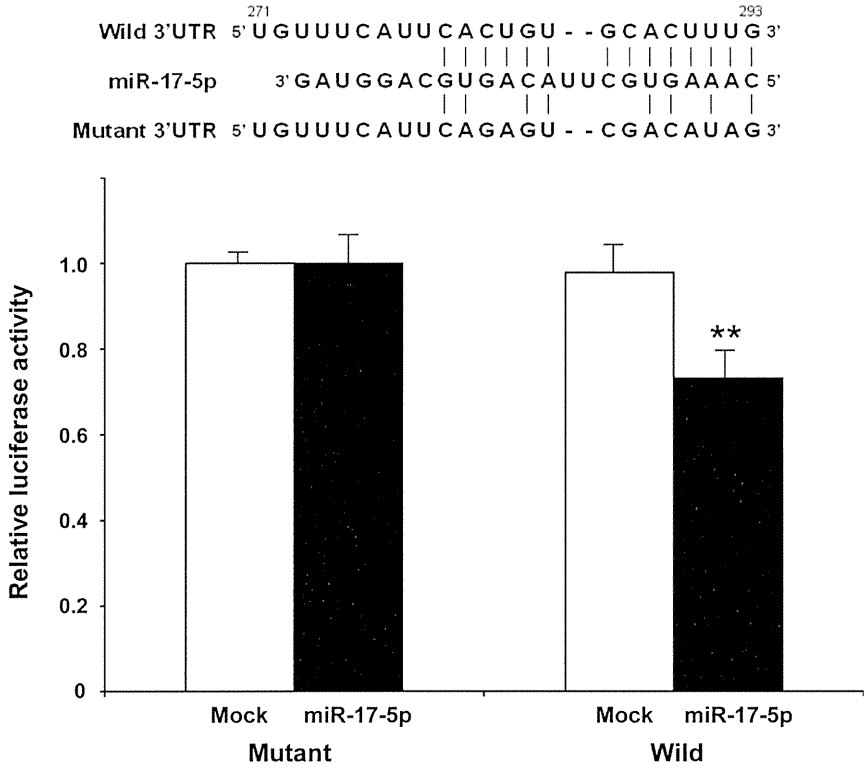


**Figure 5. Luciferase reporter assay.** miR-17-5p inhibited the luciferase activity of the wild-type MAP3K8 3'UTR construct (right), whereas no decrease in activity was observed in cells co-transfected with the mutant MAP3K8 3'UTR construct (left) or mock plus wild-type or mutant construct (right and left, respectively). Bars indicate the means of three independent experiments, and the error bars indicate standard deviations. $^{**}p<0.001$ compared with controls.
doi:10.1371/journal.pone.0097078.g005

type, patient race, treatment response definitions, study endpoints, and treatment regimens. This study analyzed patients with a homogeneous race and genotype (1b) who adhered to combination therapy and treatment for a specified duration.

MAP3K8, also known as cancer Osaka thyroid (cot) [22] or tumor progression locus 2 (tpl2) [23], was originally recognized as a proto-oncogenic protein. Toll-like receptors (TLRs) are innate immune sensors stimulated by specific microbial and viral components, including HCV. *In vitro* HCV infection directly induces TLR4 expression and activates human B cells to increase the production of IFN-β and IL-6 [24]. Peripheral blood mononuclear cells from HCV-infected individuals express higher TLR4 levels compared with uninfected controls [24]. In the IKK-NF-κB pathway, certain activated TLRs, including TLR4, induce inhibition of kappa B kinase (IKK)- catalyzed phosphorylation of nuclear factor kappa B (NF-κB) p105. Nonphosphorylated NF-κB p105 forms a stable, inactive complex with MAP3K8. Subsequent ubiquitination and proteasome-mediated processing of NF-κB-p105 to NF-κB-p50 releases MAP3K8, which activates the MAPK/ERK kinase (MEK)-extracellular signal-regulated kinase (ERK) pathway. MEK-ERK regulates the expression of pro- and anti-inflammatory mediators that lead to the production of various cytokines and chemokines in a stimulus- and cell/receptor type-specific manner (Fig. S3, Fig. S4) [25,26]. Indeed, MAP3K8 is an important and novel therapeutic target for inflammatory diseases [27]. MAP3K8 is involved in ERK signaling activation in hepatic Kupffer and stellate cells with being stimulated by TLR4 and TLR9, leading to ERK-dependent expression of the fibrogenic genes IL-1β and TIMP-1. Thus, MAP3K8 expression may contribute to liver fibrosis [28].

In addition, this study provided a novel insight into MAP3K8, which is involved in resistance to HCV treatment. The results of experiments in this study demonstrated the importance of MAP3K8 in HCV production. MAP3K8 knockdown by siRNA altered extracellular, but not intracellular, HCV core antigen levels. This result suggests that MAP3K8 might be involved in the release or assembly of HCV, does not exclude the possibility that MAP3K8 participates in intracellular HCV core production because miR-17-5p influenced both supernatant and cell-lysate HCV core antigen levels along with MAP3K8 mRNA and protein levels. If MAP3K8 limited viral release/assembly alone, intracellular HCV core antigen would accumulate following siRNA transfection. Conversely, MAP3K8 overexpression did not affect HCV production, probably because enough MAP3K8 may exist in the cells. This result is generally observed in other critical host factors (e.g. hVAP-33) involved in the HCV life cycle [29]. The above description [24–26] and *in silico* analyses (Fig. S3, Fig. S4) suggest that MAP3K8 might play a role in HCV production through a regulatory pathway and network (Fig. S5); however, the exact mechanism remains unknown and requires further investigation. It is important to note that there may be differences between the HCV genotype 1b- and 2a-derived strains/replicons. The 2a-derived JFH1 infection system is highly competent compared with other genotype-derived systems and allows steady inhibition and expression analyses [30]. Notably, this *in vitro* study focused on the correlation between MAP3K8 and miR-17-5p and their impact on HCV production; there may not be significant genotypic effect on MAP3K8 and miR-17-5p. Importantly, it is difficult to determine genotype-specific differences using different infection-competent systems.

The miR-17-92 polycistron, also known as the first oncomir, encodes six or seven miRNAs, including miR-17-5p [31,32], and is frequently overexpressed in several tumors [31,33]. In contrast, overexpression of miR-17-5p also leads to tumor suppression in breast cancer [34] and HeLa cells [32]. miR-17-5p may function as both a tumor suppressor and an oncogenic activator by targeting both pro- and anti-proliferative genes and by competing with each other in different cellular contexts, which are dependent on the expression of other transcriptional regulators [35]. Known targets of the miR-17-92 cluster primarily regulate cell cycle progression, apoptosis, and transcription factors [32,35]. Physiologically, this cluster is down-regulated during aging, and hematopoietic and lung differentiation. During HIV infection, suppression of this cluster by the virus is required for efficient viral replication [36]. Our results suggest that inhibition of miR-17-5p expression may be advantageous for HCV production. Interestingly, miR-17-5p overexpression in HeLa cells decreases the expression of the low-density lipoprotein (LDL) receptor (LDLR) and consequently induces reduced intracellular lipoprotein accumulation because of the impaired internalization [32]. LDLR is one of putative HCV receptors; however, its precise role remains controversial [37-40]. LDLR also aids the optimization of HCV replication, and the expression levels are stimulated by HCV infection. Decreased LDLR and lipoprotein uptake through LDLR may adversely affect the HCV life cycle because hepatocyte lipid metabolism pathways are required for HCV.

Bioinformatics and *in vitro* experiments showed that miR-17-5p expression levels were inversely correlated with MAP3K8 in response to anti-HCV treatment. miR-17-5p repressed HCV production by inhibiting MAP3K8 expression, whereas miR-17-5p expression was influenced by MAP3K8. The results also suggested a specific interaction between miR-17-5p and MAP3K8 3′UTR, which was previously validated by the luciferase reporter assay [35]. Taken together, MAP3K8 expression following HCV infection is negatively influenced by miR-17-5p at both the translational and transcriptional levels. This molecular interaction is a potential target for novel molecular therapeutics. However, a single miRNA can regulate the expression of multiple target mRNAs by imperfect base pairing [9,10]. Conversely, the expression of a single mRNA may be regulated by several miRNAs. Numerous mRNAs and miRNAs are key regulators in complicated pathophysiological networks (Fig. S3, Fig. S4). Therefore, it is important to note that the complex interaction between MAP3K8 and miR-17-5p may not be reflective of a correlation between their expression and viral load in our patient cohort.

Abundant hepatic miR-122 expression is essential for efficient HCV replication in cultured human hepatoma cells [11]. Suppression of miR-122 leads to a marked reduction and long-lasting suppression of HCV RNA in both sera and the livers of nonhuman primates with chronic HCV infection [41]. Paradoxically, this study showed significantly lower miRNA-122 (hsa-miR-122-5p) expression levels in null/partial responders than in SVRs/relapsers, independent of other factors. This finding is in agreement with the results of a previous study, which reported markedly low baseline miR-122 levels in poor responders [21]. Moreover, no positive correlation was observed between miR-122 expression and viral load. No convincing explanation exists for these paradoxical results. Re-analysis of registered miRNA microarray data [8] identified significantly low miR-122 levels, no change in miR-675-5p levels, and low (although not significant) miR-17-5p levels in null/partial responders. Most miR-122 target genes are involved in the lipid biogenesis pathway [42], and miR-122 antagonism induces a substantial decrease in plasma lipid levels. As described above, host lipid metabolism is vital to HCV [40], and may be related to the endogenous IFN response to HCV and IL28B SNPs [43]. However, we did not find a correlation between miR-122 expression and serum lipid levels nor identify miR-122 target genes, including lipid-related metabolic pathways, which could be considered key molecular signatures contributing to a null/partial response.

In conclusion, both global mRNA and miRNA expression profiling analyses increase our understanding of the molecular mechanisms that underlie refractory treatment responses and are even applicable to next-generation treatment. The results obtained in this study also aid the identification of novel features of known genes and target molecules for future therapeutic intervention.

## Supporting Information

**Figure S1 Hierarchical cluster analysis of mRNA expression using microarray analysis.** Changes in mRNA expression levels are presented in graduated color patches from green (least expression) to red (most abundant expression).
(TIF)

**Figure S2 Hierarchical cluster analysis of miRNA expression using microarray analysis.** Changes in gene expression are presented in graduated color patches from blue (least expression) to red (most abundant expression).
(TIF)

**Figure S3 Relationship between MAP3K8 (Tpl2/Cot) and related genes in underlying gene regulatory networks.** MAP3K8 (Tpl2/Cot) was integrated by Kyoto Encyclopedia of Genes and Genomes (KEGG) Pathways. MAP3K8 (Tpl2/Cot) was identified as an important node and considered to be a key regulator.
(TIF)

**Figure S4 Gene networks for MAP3K8 and hsa-miR-17.** MAP3K8 and hsa-miR-17 and array-independent/literature-based text-mining were integrated into the gene regulatory network analysis (Agilent Literature Search). The interaction data were visualized and analyzed by Cytoscape. MAP3K8 and its related mRNAs were associated with the miR-17 cluster family and its related miRNAs via IRF6, STAT3, AKT1, EPHB2, TIMP1, and VEGFA.
(TIF)

**Figure S5 Postulated scheme for HCV replication regulated by MAP3K8 and hsa-miR-17-5p.** IKK, inhibition of kappa B kinase; NF-κB, nuclear factor kappa B; MAP3K8, mitogen-activated protein kinase kinase kinase 8; MEK, MAPK/extracellular signal-regulated kinase.
(TIF)

**Table S1 Comparison of baseline profiles between SVRs/relapsers and null/partial responders.**
(DOC)

**Data S1 List of gene probe sets up- and down-regulated in sustained virological responders (SVR) and relapsers compared with those in null responders.**
(XLS)

**Data S2 List of microRNA probe sets up- and down-regulated in sustained virological responders (SVR) and relapsers compared with those in null responders.**
(XLS)

**Data S3 List of all gene probe sets up- and down-regulated in sustained virological responders (SVR) and**

**relapsers compared with those in null responders, and gene signatures in previously reported references.**
(XLS)

## Acknowledgments

We thank Dr. Takaji Wakita (National Institute of Infectious Diseases) for providing the JFH1-transfected cells and Haruyo Aoyagi (National Institute of Infectious Diseases), Rie Agata, and Yoko Yumoto (Jikei University School of Medicine) for their excellent technical support.

## Author Contributions

Conceived and designed the experiments: AT HA. Performed the experiments: AT HA K. Miyaguchi. Analyzed the data: AT K. Mogushi HA K. Miyaguchi TK TF HT. Contributed reagents/materials/analysis tools: AT KN HM TM TF. Wrote the paper: AT.

## References

1. Ghany MG, Nelson DR, Strader DB, Thomas DL, Seeff LB (2011) An update on treatment of genotype 1 chronic hepatitis C virus infection: 2011 practice guideline by the American Association for the Study of Liver Diseases. Hepatology 54: 1433–1444.
2. Kumada H, Toyota J, Okanoue T, Chayama K, Tsubouchi H, et al. (2012) Telaprevir with peginterferon and ribavirin for treatment-naive patients chronically infected with HCV of genotype 1 in Japan. J Hepatol 56: 78–84.
3. Hayashi N, Okanoue T, Tsubouchi H, Toyota J, Chayama K, et al. (2012) Efficacy and safety of telaprevir, a new protease inhibitor, for difficult-to-treat patients with genotype 1 chronic hepatitis C. J Viral Hepat 19: e134–142.
4. Chen L, Borozan I, Feld J, Sun J, Tannis LL, et al. (2005) Hepatic gene expression discriminates responders and nonresponders in treatment of chronic hepatitis C viral infection. Gastroenterology 128: 1437–1444.
5. Feld JJ, Nanda S, Huang Y, Chen W, Cam M, et al. (2007) Hepatic gene expression during treatment with peginterferon and ribavirin: Identifying molecular pathways for treatment response. Hepatology 46: 1548–1563.
6. Sarasin-Filipowicz M, Oakeley EJ, Duong FH, Christen V, Terracciano L, et al. (2008) Interferon signaling and treatment outcome in chronic hepatitis C. Proc Natl Acad Sci USA 105: 7034–7039.
7. Honda M, Sakai A, Yamashita T, Nakamoto Y, Mizukoshi E, et al. (2010) Hepatic ISG expression is associated with genetic variation in interleukin 28B and the outcome of IFN therapy for chronic hepatitis C. Gastroenterology 139: 499–509.
8. Murakami Y, Tanaka M, Toyoda H, Hayashi K, Kuroda M, et al. (2010) Hepatic microRNA expression is associated with the response to interferon treatment of chronic hepatitis C. BMC Med Genomics 3: 48.
9. Lim LP, Lau NC, Garrett-Engele P, Grimson A, Schelter JM, et al. (2005) Microarray analysis shows that some microRNAs downregulate large numbers of target mRNAs. Nature 433: 769–773.
10. Selbach M, Schwänhausser B, Thierfelder N, Fang Z, Khanin R, et al. (2008) Widespread changes in protein synthesis induced by microRNAs. Nature 455: 58–63.
11. Jopling CL, Yi M, Lancaster AM, Lemon SM, Sarnow P (2005) Modulation of hepatitis C virus RNA abundance by a liver-specific MicroRNA. Science 309: 1577–1581.
12. Gottwein E, Cullen BR (2008) Viral and cellular microRNAs as determinants of viral pathogenesis and immunity. Cell Host Microbe 3: 375–387.
13. Desmet VJ, Gerber M, Hoofnagle JH, Manns M, Scheuer PJ (1994) Classification of chronic hepatitis: diagnosis, grading and staging. Hepatology 19: 1513–1520.
14. Zhong J, Gastaminza P, Cheng G, Kapadia S, Kato T, et al. (2005) Robust hepatitis C virus infection in vitro. Proc Natl Acad Sci USA 102: 9294–9299.
15. Wakita T, Pietschmann T, Kato T, Date T, Miyamoto M, et al. (2005) Production of infectious hepatitis C virus in tissue culture from a cloned viral genome. Nat Med 11: 791–796.
16. Ge D, Fellay J, Thompson AJ, Simon JS, Shianna KV, et al. (2009) Genetic variation in IL28B predicts hepatitis C treatment-induced viral clearance. Nature 461: 399–401.
17. Tanaka Y, Nishida N, Sugiyama M, Kurosaki M, Matsuura K, et al. (2009) Genome-wide association of IL28B with response to pegylated interferon-alpha and ribavirin therapy for chronic hepatitis C. Nat Genet 41: 1105–1109.
18. Fellay J, Thompson AJ, Ge D, Gumbs CE, Urban TJ, et al. (2010) ITPA gene variants protect against anaemia in patients treated for chronic hepatitis C. Nature 464: 405–408.
19. Urban TJ, Thompson AJ, Bradric SS, Fellay J, Schuppan D, et al. (2010) IL28B genotype is associated with differential expression of intrahepatic interferon-stimulated genes in patients with chronic hepatitis C. Hepatology 52: 1888–1896.
20. Dill MT, Duong FHT, Vogt JE, Bibert S, Bochud PY, et al. (2011) Interferon-induced gene expression is a stronger predictor of treatment response than IL28B genotype in patients with hepatitis C. Gastroenterology 140: 1021–1031.
21. Sarasin-Filipowicz M, Krol J, Markiewicz I, Heim MH, Filipowicz W (2009) Decreased levels of microRNA miR-122 in individuals with hepatitis C responding poorly to interferon therapy. Nat Med 15: 31–33.
22. Miyoshi J, Higashi T, Mukai H, Ohuchi T, Kakunaga T (1991) Structure and transforming potential of the human cot oncogene encoding a putative protein kinase. Mol Cell Biol 11: 4088–4096.
23. Patriotis C, Makris A, Bear SE, Tsichlis PN (1993) Tumor progression locus 2 (Tpl-2) encodes a protein kinase involved in the progression of rodent T-cell lymphomas and in T-cell activation. Proc Natl Acad Sci USA 90: 2251–2255.
24. Machida K, Cheng KT, Sung VM, Levine AM, Foung S, et al. (2006) Hepatitis C virus induces toll-like receptor 4 expression, leading to enhanced production of beta interferon and interleukin-6. J Virol 80: 866–874.
25. Banerjee A, Gerondakis S (2007) Coordinating TLR-activated signaling pathways in cells of the immune system. Immunol Cell Biol 85: 420–424.
26. Gantke T, Sriskantharajah S, Sadowski M, Ley SC (2012) IκB kinase regulation of the TPL-2/ERK MAPK pathway. Immunol Rev 246: 168–182.
27. George D, Salmeron A (2009) Cot/Tpl-2 protein kinase as a target for the treatment of inflammatory disease. Curr Top Med Chem 9: 611–622.
28. Perugorria MJ, Murphy LB, Fullard N, Chakraborty JB, Vyrla D, et al. (2013) Tpl2/Cot is required for activation of ERK in liver injury and TLR induced TIMP-1 gene transcription in hepatic stellate cells. Hepatology 57: 1238–1249.
29. Gao L, Aizaki H, He JW, Lai MM (2004) Interactions between viral nonstructural proteins and host protein hVAP-33 mediate the formation of hepatitis C virus RNA replication complex on lipid raft. J Virol 78: 3480–3488.
30. Kato T, Matsumura T, Heller T, Saito S, Sapp RK, et al. (2007) Production of infectious hepatitis C virus of various genotypes in cell cultures. J Virol 81: 4405–4411.
31. He L, Thomson JM, Hemann MT, Hernando-Monge E, Mu D, et al. (2005) A microRNA polycistron as a potential human oncogene. Nature 435: 828–833.
32. Serva A, Knapp B, Tsai YT, Claas C, Lisauskas T, et al. (2012) miR-17-5p regulates endocytic trafficking through targeting TBC1D2/Armus. PLoS One 7: e52555.
33. Volinia S, Calin GA, Liu CG, Ambs S, Cimmino A, et al. (2006) A microRNA expression signature of human solid tumors defines cancer gene targets. Proc Natl Acad Sci USA 103: 2257–2261.
34. Hossain A, Kuo MT, Saunders GF (2006) Mir-17-5p regulates breast cancer cell proliferation by inhibiting translation of AIB1 mRNA. Mol Cell Biol 26: 8191–8201.
35. Cloonan N, Brown MK, Steptoe AL, Wani S, Chan WL, et al. (2008) The miR-17-5p microRNA is a key regulator of the G1/S phase cell cycle transition. Genome Biol 9: R127.
36. Triboulet R, Mari B, Lin YL, Chable-Bessia C, Bennasser Y, et al. (2007) Suppression of microRNA-silencing pathway by HIV-1 during virus replication. Science 315: 1579–1582.
37. Albecka A, Belouzard S, Op de Beeck A, Descamps V, Goueslain L, et al. (2012) Role of low-density lipoprotein receptor in the hepatitis C virus life cycle. Hepatology 55: 998–1007.
38. Bassendine MF, Sheridan DA, Bridge SH, Felmlee DJ, Neely RD (2013) Lipids and HCV. Semin Immunopathol 35: 87–100.
39. Schaefer EA, Chung RT (2013) HCV and host lipids: an intimate connection. Semin Liver Dis 33: 358–368.
40. Syed GH, Tang H, Khan M, Hassanein T, Liu J, et al. (2014) Hepatitis C virus stimulates low-density lipoprotein receptor expression to facilitate viral propagation. J Virol 88: 2519–2529.
41. Lanford RE, Hildebrandt-Eriksen ES, Petri A, Persson R, Lindow M, et al. (2010) Therapeutic silencing of microRNA-122 in primates with chronic hepatitis C virus infection. Science 327: 198–201.
42. Krützfeldt J, Rajewsky N, Braich R, Rajeev KG, Tuschl T, et al. (2005) Silencing of microRNAs in vivo with 'antagomirs'. Nature 438: 685–689.
43. Li JH, Lao XQ, Tillmann HL, Rowell J, Patel K, et al. (2010) Interferon-lambda genotype and low serum low-density lipoprotein cholesterol levels in patients with chronic hepatitis C infection. Hepatology 51: 1904–1911.

Biochemical and Biophysical Research Communications 443 (2014) 808–813

Contents lists available at ScienceDirect

Biochemical and Biophysical Research Communications

journal homepage: www.elsevier.com/locate/ybbrc

# Evaluation and identification of hepatitis B virus entry inhibitors using HepG2 cells overexpressing a membrane transporter NTCP ☆

Masashi Iwamoto [a,b], Koichi Watashi [a,b,*], Senko Tsukuda [a,c], Hussein Hassan Aly [a], Masayoshi Fukasawa [d], Akira Fujimoto [a], Ryosuke Suzuki [a], Hideki Aizaki [a], Takayoshi Ito [e], Osamu Koiwai [b], Hiroyuki Kusuhara [f], Takaji Wakita [a]

[a] Department of Virology II, National Institute of Infectious Diseases, Tokyo 162-8640, Japan
[b] Department of Applied Biological Science, Tokyo University of Sciences, Noda 278-8510, Japan
[c] Micro-signaling Regulation Technology Unit, RIKEN Center for Life Science Technologies, Wako 351-0198, Japan
[d] Department of Biochemistry and Cell Biology, National Institute of Infectious Diseases, Tokyo 162-8640, Japan
[e] Division of Gastroenterology, Department of Medicine, Showa University School of Medicine, Tokyo 142-8666, Japan
[f] The University of Tokyo, Graduate School of Pharmaceutical Sciences, Tokyo 113-0033, Japan

ARTICLE INFO

*Article history:*
Received 24 November 2013
Available online 14 December 2013

*Keywords:*
HBV
Infection
NTCP
DMSO
Cyclosporin
Oxysterol

ABSTRACT

Hepatitis B virus (HBV) entry has been analyzed using infection-susceptible cells, including primary human hepatocytes, primary tupaia hepatocytes, and HepaRG cells. Recently, the sodium taurocholate cotransporting polypeptide (NTCP) membrane transporter was reported as an HBV entry receptor. In this study, we established a strain of HepG2 cells engineered to overexpress the human NTCP gene (HepG2-hNTCP-C4 cells). HepG2-hNTCP-C4 cells were shown to be susceptible to infection by blood–borne and cell culture-derived HBV. HBV infection was facilitated by pretreating cells with 3% dimethyl sulfoxide permitting nearly 50% of the cells to be infected with HBV. Knockdown analysis suggested that HBV infection of HepG2-hNTCP-C4 cells was mediated by NTCP. HBV infection was blocked by an anti-HBV surface protein neutralizing antibody, by compounds known to inhibit NTCP transporter activity, and by cyclosporin A and its derivatives. The infection assay suggested that cyclosporin B was a more potent inhibitor of HBV entry than was cyclosporin A. Further chemical screening identified oxysterols, oxidized derivatives of cholesterol, as inhibitors of HBV infection. Thus, the HepG2-hNTCP-C4 cell line established in this study is a useful tool for the identification of inhibitors of HBV infection as well as for the analysis of the molecular mechanisms of HBV infection.



## 1. Introduction

Approximately 350 million people are estimated to be infected with hepatitis B virus (HBV) worldwide [1–4]. Chronically infected patients are at a greater risk of developing hepatocellular carcinoma. Currently, clinical treatment for HBV infection includes interferon (IFN)α and nucleos(t)ide analogs [2,4]. IFNα therapy yields long-term clinical benefit in less than 40% of the treated patients and can cause significant side effects. Nucleos(t)ide analog treatment can suppress HBV replication with substantial biochemical and histological improvement; however, such analogs may select drug-resistant viruses, thereby limiting the efficacy of long-term treatment. Thus, the development of new anti-HBV agents targeting a different molecule in the HBV life cycle is urgently needed.

HBV is a hepatotropic virus that mainly or exclusively infects human liver [1,5]. HBV infection can be reproduced in cell culture using primary human hepatocytes (PHH), primary tupaia hepatocytes (PTH), and HepaRG cells [6]. Although HBV infection into these cells is robust, these models have significant limitations as tools for analyzing the mechanisms of HBV infection. Notably, these models can yield unstable reproducibility among lots and low tolerability of transfection efficiency with plasmid and siRNA: preparation and culturing of these cells require significant

*Abbreviations:* Ab, antibody; cccDNA, covalently closed circular DNA; Cs, cyclosporin; DMSO, dimethyl sulfoxide; GEq, genome equivalent; HBc, HBV core protein; HBs, HBV surface protein; HBV, hepatitis B virus; NTCP, sodium taurocholate cotransporting polypeptide; OHC, hydroxycholesterol; PHH, primary human hepatocytes; PTH, primary tupaia hepatocytes.



* Corresponding author at: Department of Virology II, National Institute of Infectious Diseases, 1-23-1 Toyama, Shinjuku-ku, Tokyo 162-8640, Japan. Fax: +81 3 5285 1161.
*E-mail address:* kwatashi@nih.go.jp (K. Watashi).

0006-291X/$ - see front matter © 2013 The Authors. Published by Elsevier Inc. All rights reserved.
http://dx.doi.org/10.1016/j.bbrc.2013.12.052

technical skill. In the case of hepatitis C virus (HCV), development of the HCV cell culture (HCVcc) system, in which HCV produced from a JFH-1 strain-based molecular clone can reinfect Huh-7 cells, greatly contribute to the characterization of the HCV life cycle and the evaluation of novel anti-HCV drug candidates [7]. However, the above-noted limitations of HBV-susceptible cells have hampered analysis of the HBV life cycle and impeded identification of new anti-HBV drug targets. Thus, establishment of a novel cell line supporting HBV infection is expected to accelerate the molecular analyses of HBV infection as well as the development of anti-HBV agents.

Recently, the sodium taurocholate cotransporting polypeptide (NTCP) membrane transporter was reported as an HBV entry receptor [8]. NTCP is a sodium-dependent transporter for taurocholic acid, and belongs to a family of solute carrier proteins that consist of seven members (SLC10A1-A7) [9,10]. NTCP is expressed at the basolateral membrane of hepatocytes and mediates the transport of conjugated bile acids and some drugs from portal blood to the liver [11]. NTCP specifically interacts with the large surface protein of HBV, thereby functioning as a viral entry receptor [8].

In this study, we established a strain of HepG2 cells engineered to overexpress the NTCP-encoding gene. One of these clones, designated HepG2-hNTCP-C4, was shown to be highly susceptible for HBV infection, confirming that this infection is mediated by NTCP and permitting evaluation in these cells of the anti-HBV activity of various compounds: reduction of HBV infection of HepG2-hNTCP-C4 cells was observed upon treatment with compounds that blocked HBV entry in other assays and by known inhibitors of NTCP transporter activity [12]. A small-scale chemical screen permitted use to identify oxysterols as inhibitors of HBV infection. Thus, the cell line established in this study is useful for screening for anti-HBV agents, as well as for analysis of the molecular mechanisms of HBV infection.

## 2. Materials and methods

### 2.1. Reagents

Dimethyl sulfoxide (DMSO), anti-FLAG antibody (Ab), dextran sulfate, cholate, progesterone, 22(S)-hydroxycholesterol (OHC), 25-OHC, 20α-OHC, and 7β-OHC were purchased from Sigma. Ursodeoxycholate was purchased from Tokyo Chemical Industry. Bromosulfophthalein was from MP biomedicals. Cyclosporin (Cs)A, CsB, CsC, CsD, and CsH were obtained from Enzo Lifesciences. Anti-HBV surface protein (HBs) Ab was from Abcam. Heparin was obtained from Mochida Pharmaceuticals. Myrcludex-B was kindly provided by Dr. Stephan Urban at University Hospital Heidelberg and was synthesized by CS Bio (Shanghai, China).

### 2.2. Cell culture and plasmid transfection

HepG2 and HepG2-hNTCP-C4 cells were cultured with DMEM/F-12 + GlutaMax (Invitrogen) supplemented with 10 mM HEPES (Invitrogen), 200 units/ml penicillin, 200 μg/ml streptomycin, 10% FBS, 50 μM hydrocortisone and 5 μg/ml insulin in the presence (HepG2-hNTCP-C4 cells) or absence (HepG2 cells) of 400 μg/ml G418 (Nacalai). HepAD38 (kindly provided by Dr. Christoph Seeger at Fox Chase Cancer Center) [13] and HepaRG cells (BIOPREDIC) were cultured as described previously [14].

An expression plasmid for hNTCP [15] was transfected into HepG2 cells with TransIT-LT1 (Mirus) according to the manufacturer's instruction to establish HepG2-hNTCP-C4 cells.

### 2.3. HBV preparation and infection

HBV was prepared and infected as described [14]. Except as noted, the HBV used in this study was genotype D derived from HepAD38 cells [13]. HBV was infected into NTCP-expressing HepG2 cells at $6 \times 10^3$ or $1.8 \times 10^4$ genome equivalent (GEq)/cell or into HepaRG cells at $6 \times 10^3$ GEq/cell. All infections were performed in the presence of 4% PEG8000 at 37 °C for 16 h as previously described [14]. Dr. Urban's group reported that a quantity of more than $10^4$ GEq/cell (i.e. $1.25 - 40 \times 10^4$ GEq/cell) of HBV derived from HepAD38 or HepG2.2.15 cells was required as an inoculum for efficient infection into HepaRG cells in the presence of 4% PEG8000 [16]. A limited number of infections were performed with HBV of genotype C, derived from the serum of an HBV-infected patient, at 100 GEq/cell.

### 2.4. Real-time PCR and RT-PCR

Real-time PCR for quantification of HBV covalently closed circular (ccc)DNA were performed as described [14]. Isolation of total RNA from cell lysates and reverse transcription PCR (RT-PCR) using a One step RNA PCR kit (Takara) were performed as described previously [17]. Primers used in this study were as follows: 5′-AGGGAGGAGGTGGCAATCAAGAGTGG-3′ and 5′-CCGGCTGAAGAACATTGAGGCACTGG-3′ for NTCP, 5′-CCATGGAGAAGGCTGGGG-3′ and 5′-CAAAGTTGTCATGGATGACC-3′ for GAPDH, respectively.

### 2.5. Detection of HBs and HBe antigens

HBs antigen was quantified by ELISA as described previously [14]. HBe antigen was detected by Chemiluminescent Immuno Assay (Mitsubishi Chemical Medience).

### 2.6. Southern blot analysis

Isolation of cellular DNA and southern blot analysis to detect HBV DNAs were performed as described previously [14].

### 2.7. Indirect immunofluorescence analysis

Immunofluorescence was conducted essentially as described [14] using an anti-HBc Ab (#B0586, DAKO) at a dilution of 1:1000.

### 2.8. Flow cytometry

An aliquot of $1 \times 10^6$ of HepG2 or HepG2-hNTCP-C4 cells was incubated for 30 min with a 1:50 dilution of anti-NTCP Ab (Abcam), then washed and incubated with a dye-labeled secondary Ab (Alexa Fluor 488, Invitrogen) at 1:500 dilution in the dark. Staining and washing were carried out at 4 °C in PBS supplemented with 0.5% bovine serum albumin and 0.1% sodium azide. The signals were analyzed with Cell Sorter SH8000 (SONY).

### 2.9. siRNA transfection

siRNAs were transfected into the cells at a final concentration of 10–30 nM using Lipofectamine RNAiMAX (Invitrogen) according to the manufacturer's protocol. siRNAs were purchased from Sigma.

### 2.10. Statistical analyses

Statistical analyses are done with student *t*-test.

## 3. Results and discussion

### 3.1. Establishment of a cell line susceptible to HBV infection

To establish a cell line permanently expressing NTCP, we transfected an NTCP-encoding plasmid into HepG2 cells and selected with G418 at 1 mg/ml for 3 weeks. The resultant 9 cell clones were isolated and NTCP expression was analyzed by RT-PCR. One of these clones, designated HepG2-hNTCP-C4, was used in the following experiments because this specific clone exhibited high expression of NTCP and high susceptibility to HBV infection, as shown below. Specifically, NTCP mRNA was abundantly expressed in HepG2-hNTCP-C4 cells, in contrast to little to no expression of NTCP mRNA in the parental HepG2 cells (Fig. 1A). Consistent with the mRNA levels, NTCP protein was detected on the cell surface in HepG2-hNTCP-C4 cells (Fig. 1B). To evaluate HBV infection, these cells were inoculated with HBV for 16 h and cultured in normal growth medium for an additional 12 days, and then HBV surface protein (HBs) and HBe antigens in the culture supernatant as well as HBV DNAs, covalently closed circular (ccc)DNA, and HBV core (HBc) in the cells were assessed. The HBV inoculum used in this experiment was of genotype D, and was derived from the culture supernatant of HepAD38 cells that produce HBV by depletion of tetracycline [13]. To confirm that the detected signals were derived from HBV infection and did not represent non-specific background, the cells were incubated with 1 μM Myrcludex-B (or with DMSO vehicle) for 3 h prior to and for 16 h during HBV infection. Myrcludex-B is a lipopeptide consisting of amino acid residues 2–48 of the pre-S1 region of HBV, and is known to block HBV entry [18]. Following HBV exposure, little or no HBs and HBe antigens was detected in the culture supernatant of the parental HepG2 cells, and little HBc protein was observed in these cells (Fig. 1C, D, and G). However, these proteins, as well as HBV DNAs and cccDNA, were detected in HBV-treated HepG2-hNTCP-C4 cells (Fig. 1C–G). The corresponding signals were significantly reduced in the cells treated with an HBV entry inhibitor, Myrcludex-B, but not in the cells treated with DMSO (Fig. 1C–G). These data suggested that HepG2-hNTCP-C4 cells are HBV-susceptible, in contrast to the parental HepG2 cells. The HepG2-hNTCP-C4 cell line also was susceptible to infection with HBV genotype C, which was derived from the serum of an HBV-infected patient (Fig. 1H and I).

### 3.2. HBV susceptibility of HepG2-hNTCP-C4 cells was augmented by pretreatment with DMSO

It has been reported that a prolonged HBV infection in primary human hepatocytes can be enhanced by pretreatment with DMSO [19]. Therefore, we examined whether pretreatment with DMSO affected HBV infection of HepG2-NTCP-C4 cells. The cells were pretreated with 3% DMSO for 24 h and then the HBV infectivity was investigated following the protocol as in Fig. 1. Immunofluorescence analysis revealed that approximately 50% of the DMSO-pretreated cells were HBc-positive at 12 days post-infection (Fig. 2A, middle), while only 10–20% of cells were HBc-positive cells in the absence of pretreatment (Fig. 1G, upper right). The effect of DMSO pretreatment on HBV susceptibility was both concentration-(Fig. 2B) and time-dependent (Fig. 2C).

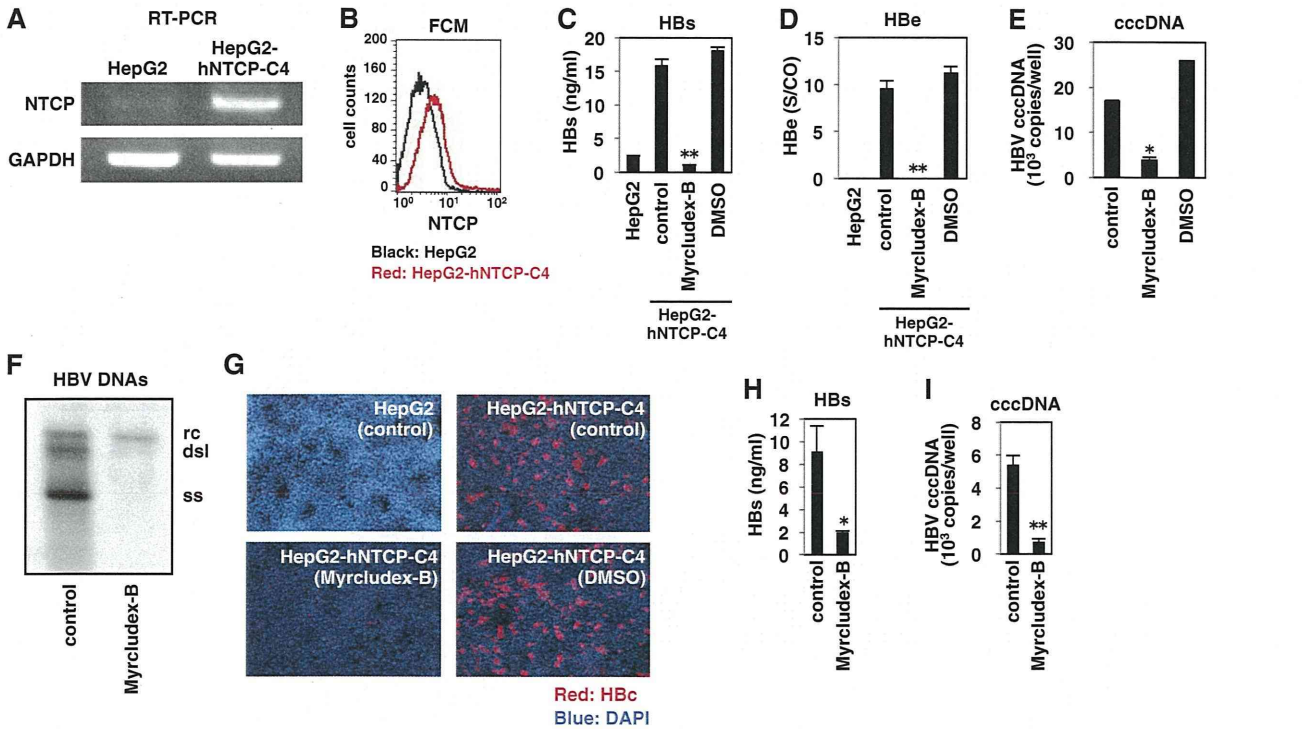


**Fig. 1.** Establishment of a cell line susceptible to hepatitis B virus (HBV) infection. (A) mRNAs for sodium taurocholate cotransporting polypeptide (NTCP) and GAPDH in HepG2 and HepG2-hNTCP-C4 cells were detected by RT-PCR. (B) NTCP protein on cell surface of HepG2 (black) and HepG2-hNTCP-C4 cells (red) was detected by flow cytometry. (C-G) HepG2-hNTCP-C4 or the parental HepG2 cells pretreated with or without 1 μM Myrcludex-B or vehicle (DMSO) for 3 h were inoculated with HBV (genotype D) for 16 h. After washing out of the free virus and the compounds, the cells were cultured for an additional 12 days in normal growth medium and then assayed for secretion of HBs (C) and HBe antigens (D) secreted in the culture supernatant, and for the presence of HBV covalently closed circular (ccc)DNA (E), HBV DNAs (F), and HBV core (HBc) proteins (G) in the cells. rc, dsl, and ss in (F) indicate relaxed circular, double strand linear, and single strand HBV DNA, respectively. Red and blue signals in (G) indicate HBc protein and nuclear staining, respectively. (H and I) Infection of blood–borne HBV into HepG2-hNTCP-C4 cells. HBV (genotype C) derived from an HBV-infected patient was used as an inoculum for the infection assay. Levels for HBs antigen in the culture supernatant (H) and HBV cccDNA in the cells (I) are shown. The data in C–E, H, and I show the means of three independent experiments. $^{*}P < 0.05$, $^{**}P < 0.01$.

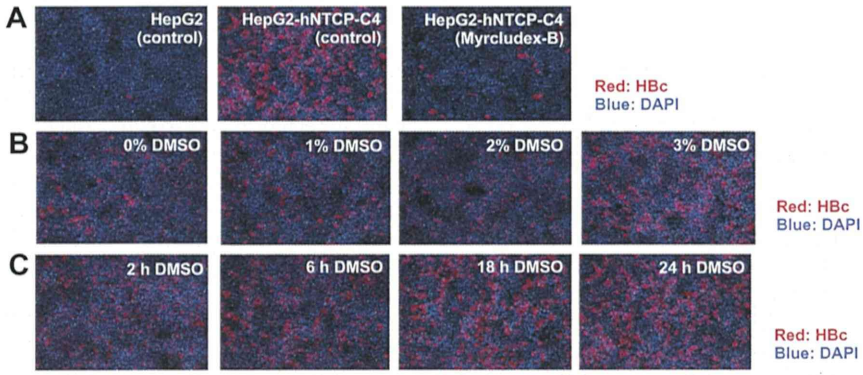


**Fig. 2.** HBV infection was facilitated by pretreatment of HepG2-hNTCP-C4 cells with DMSO. (A) HepG2 or HepG2-hNTCP-C4 cells preincubated with 3% DMSO for 24 h were inoculated with HBV in the presence of 3% DMSO for 16 h. Treatment with Myrcludex-B was used as a negative control for infection. At 12 days postinfection, HBc protein (red) and the nucleus (blue) were detected by immunofluorescence analysis. (B) Cells were pretreated by exposure for 24 h to various concentrations of DMSO (0–3%). (C) Cells were pretreated by exposure to 3% DMSO for various treatment times (2, 6, 18, and 24 h). HBc protein (red) and the nucleus (blue) were detected as in (A).

### 3.3. HBV infection was mediated by NTCP in HepG2-hNTCP-C4 cells

We used knockdown analysis to determine whether HBV infection of HepG2-hNTCP-C4 cells was mediated by NTCP. Transfection with siRNA against NTCP (si-NTCP) and GAPDH (si-GAPDH) specifically knocked down mRNA for NTCP and GAPDH, respectively, in HepG2-hNTCP-C4 cells (Fig. 3A). Consistent with the effect on transcript level, treatment with si-NTCP depleted NTCP protein on the cell surface (Fig. 3B). The HBV infection assay, performed as in Fig. 1, indicated that depletion of NTCP reduced the levels for HBs (Fig. 3C) and HBe antigens (Fig. 3D) in culture supernatant as well as HBV cccDNA (Fig. 3E) and HBc protein (Fig. 3F) in the cells at 12 days postinfection with HBV. These data suggested that HBV infection into HepG2-hNTCP-C4 cells was mediated by NTCP.

### 3.4. Evaluation of HBV entry inhibitors in HepG2-hNTCP-C4 cells

To determine whether HepG2-hNTCP-C4 cells could be used to evaluate anti-HBV activity of compounds, we examined the effect of known entry inhibitors in these cells. The cells were pretreated with compounds for 3 h and then inoculated with HBV for 16 h in the presence of compounds (Fig. 4A). Inoculation with HBV was followed by culturing of the cells in normal growth medium for an additional 12 days until detection of HBs antigen in the culture supernatant and cccDNA in the cells (Fig. 4A). This protocol has been used previously to evaluate the entry inhibition activity of compounds [20]. Treatment with anti-HBs neutralizing Ab, but not that with a non-relevant anti-FLAG Ab, inhibited HBV infection (Fig. 4B). Heparin and dextran sulfate, which have been reported to inhibit HBV attachment to the target cells [21], also reduced HBV infection (Fig. 4C). In addition, known NTCP substrates and inhibitors, including ursodeoxycholate, cholate, progesterone, and bromosulfophthalein [12], blocked HBV infection in this assay (Fig. 4D). We recently identified that cyclosporin A (CsA) and its analogs blocked HBV entry through inhibition of interaction between NTCP and the HBV large surface protein [20]. As shown in Fig. 4E, CsA and its analogs inhibited HBV infection in the present assay, with CsB showing the highest potency for inhibition of HBV infection among Cs analogs (Fig. 4E). These data indicate that HepG2-hNTCP-C4 cells are useful for evaluating the effect of HBV entry inhibitors.

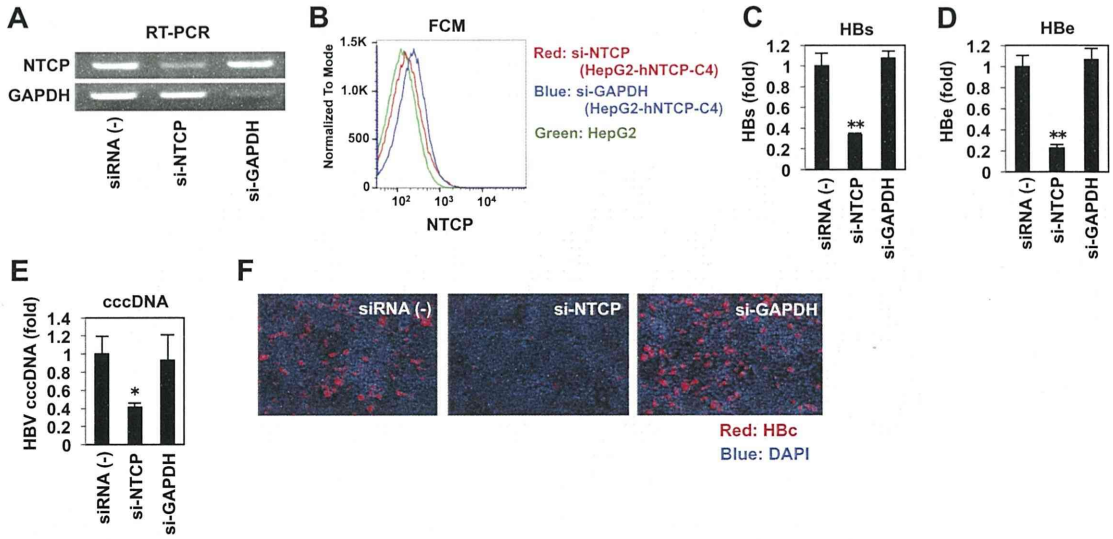


**Fig. 3.** HBV infection of HepG2-hNTCP-C4 cells was mediated by NTCP. (A) HepG2-hNTCP-C4 cells were transfected (for 48 h) with or without [siRNA(−)] siRNAs against NTCP (si-NTCP) or GAPDH (si-GAPDH), and mRNA expression levels of NTCP and GAPDH were detected by RT-PCR. (B) Parental HepG2 and HepG2-hNTCP-C4 cells were transfected (for 48 h) with or without si-NTCP or si-GAPDH, and cell surface-displayed NTCP protein was detected by flow cytometry. The red, blue, and green lines indicate the signal in HepG2-hNTCP-C4 cells treated with si-NTCP, HepG2-hNTCP-C4 cells treated with si-GAPDH, and HepG2 cells, respectively. (C–F) The cells prepared as in (A) were infected with HBV according to the protocol shown in Fig. 1. Culture supernatants were assayed for levels of secreted HBs (C) and HBe (D) antigens, and cells were assayed for intracellular levels of HBV cccDNA (E) and HBc protein (F). The red and blue signals in (F) indicate HBc and nuclear staining, respectively.

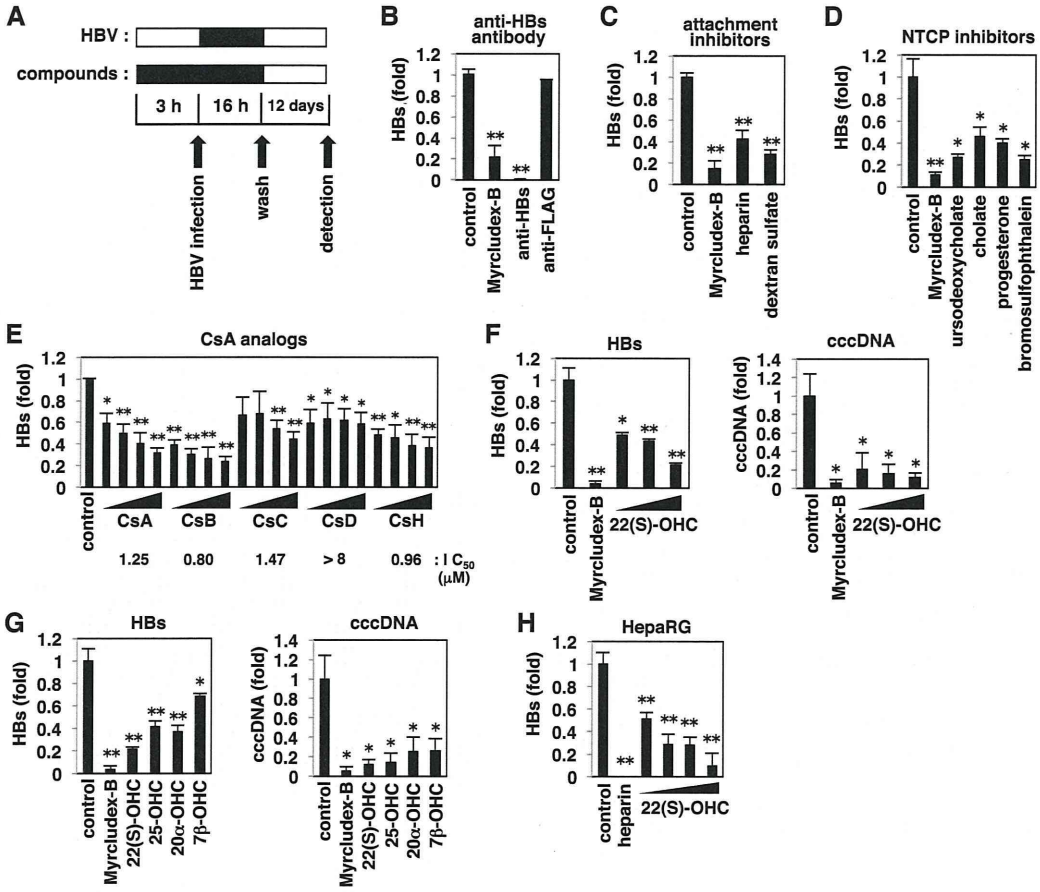


**Fig. 4.** Evaluation of HBV entry inhibitors in HepG2-hNTCP-C4 cells. (A) Schematic representation of the experimental procedure for evaluating HBV entry inhibition. HepG2-hNTCP-C4 cells were pretreated with or without compounds for 3 h and then inoculated with HBV for 16 h. After washing out of free HBV and the compounds, the cells were cultured with normal culture medium in the absence of compounds for an additional 12 days, and HBs antigen in the culture supernatant and/or HBV cccDNA in the cells were detected. Black and white bars show period of treatment and without treatment, respectively. (B–G) HepG2-hNTCP-C4 cells were treated with or without 1 μM Myrcludex-B, 10 μg/ml anti-HBs or anti-FLAG Ab (B); HBV attachment inhibitors including 100 IU/ml heparin and 1 mg/ml dextran sulfate (C); NTCP inhibitors including 100 μM ursodeoxycholate, 100 μM cholate, 40 μM progesterone, and 100 μM bromosulfophthalein (D); cyclosporins (CsA, CsB, CsC, CsD, CsH) at 1, 2, 4, and 8 μM (E); 22(S)-hydroxycholesterol (OHC) at 11, 33, and 100 μM (F); or oxysterols including 22(S)-OHC, 25-OHC, 20α-OHC, and 7β-OHC at 100 μM (G). For each assay, the cells were infected with HBV as shown in (A) and the levels of HBs antigen secreted into the culture supernatant and/or cccDNA in the cells were detected. Pretreatment time of compounds in (F) and (G) was 6 h, instead of 3 h. $IC_{50}$s of cyclosporin derivatives calculated in this assay are shown below the graph in (E). (H) HepaRG cells were treated with or without various concentrations of 22(S)-OHC (0.3, 0.9, 3, and 9 μM) and infected with HBV according to the protocol shown in (A). HBV infection was monitored by detecting the level of HBs secreted into the culture supernatant.

As there are only reverse transcriptase inhibitors currently available as anti-HBV drugs that inhibit the HBV life cycle, development of new anti-HBV agents targeting different steps in the HBV life cycle are greatly needed [1–4]. We therefore screened for compounds that blocked HBV entry by following the same protocol as in Fig. 4A. We found that an oxysterol, 22(S)-hydroxycholesterol (OHC), reduced HBV infection in a dose-dependent manner (Fig. 4F). Other oxysterols, 25-OHC, 20α-OHC, and 7β-OHC, also significantly decreased HBV infection (Fig. 4G). To validate this result, we repeated the assay using HepaRG cells, a line that frequently has been used in HBV entry experiments [14]. We found that 22(S)-OHC also reduced HBV infection of HepaRG cells in a dose-dependent manner (Fig. 4H), suggesting that the observed inhibitory effect of oxysterols reflects a genuine inhibition of HBV infection.

Thus, we have newly established a cell line that is susceptible to HBV infection. HepG2-hNTCP-C4 cells exhibited approximately 50% of HBV-infection positive cells (Fig. 2A), while maximum HBV infection of HepaRG cells was reported to be only 7% [16] or 20% [22] of the total population. These cells are expected to be useful for analyzing the molecular mechanisms of HBV infection, given that HepG2-derived cells show higher efficiency of transfection with expression plasmids and siRNAs than the current available HBV-susceptible PHH, PTH, and HepaRG cells. HepG2-hNTCP-C4 cells will facilitate knockdown analysis of host factors to define their roles in infection and screenings of compounds to identify novel inhibitors of HBV infection. As an example, we demonstrated here that oxysterols blocked HBV infection. The molecular mechanisms whereby oxysterols inhibit HBV infection are now under investigation. These analyses will be important for understanding the mechanisms of HBV infection as well as for developing new anti-HBV agents.

## Acknowledgments

HepAD38 cells were kindly provided by Dr. Christoph Seeger at Fox Chase Cancer Center. Myrcludex-B, a pre-S1 lipopeptide, was kindly provided by Dr. Stephan Urban at University Hospital Heidelberg. We also are grateful to all of the members of Department of Virology II, National Institute of Infectious Diseases. This study was supported by Grants-in-aid from the Ministry of Health, Labor, and Welfare, Japan, from the Ministry of Education, Culture, Sports, Science, and Technology, Japan, and from Japan Society for the Promotion of Science, and from the Research on Health Sciences Focusing on Drug Innovation from the Japan Health Sciences Foundation.

## References


[1] D. Grimm, R. Thimme, H.E. Blum, HBV life cycle and novel drug targets, Hepatol. Int. 5 (2011) 644–653.

[2] J.M. Pawlotsky, G. Dusheiko, A. Hatzakis, D. Lau, G. Lau, T.J. Liang, S. Locarnini, P. Martin, D.D. Richman, F. Zoulim, Virologic monitoring of hepatitis B virus therapy in clinical trials and practice: recommendations for a standardized approach, Gastroenterology 134 (2008) 405–415.

[3] M. Rapicetta, C. Ferrari, M. Levrero, Viral determinants and host immune responses in the pathogenesis of HBV infection, J. Med. Virol. 67 (2002) 454–457.

[4] F. Zoulim, Hepatitis B virus resistance to antiviral drugs: where are we going?, Liver Int 31 (Suppl. 1) (2011) 111–116.

[5] P. Gripon, S. Rumin, S. Urban, J. Le Seyec, D. Glaise, I. Cannie, C. Guyomard, J. Lucas, C. Trepo, C. Guguen-Guillouzo, Infection of a human hepatoma cell line by hepatitis B virus, Proc. Natl. Acad. Sci. USA 99 (2002) 15655–15660.

[6] D. Glebe, S. Urban, Viral and cellular determinants involved in hepadnaviral entry, World J. Gastroenterol. 13 (2007) 22–38.

[7] J.M. Gottwein, J. Bukh, Cutting the gordian knot-development and biological relevance of hepatitis C virus cell culture systems, Adv. Virus Res. 71 (2008) 51–133.

[8] H. Yan, G. Zhong, G. Xu, W. He, Z. Jing, Z. Gao, Y. Huang, Y. Qi, B. Peng, H. Wang, L. Fu, M. Song, P. Chen, W. Gao, B. Ren, Y. Sun, T. Cai, X. Feng, J. Sui, W. Li, Sodium taurocholate cotransporting polypeptide is a functional receptor for human hepatitis B and D virus, Elife 1 (2012) e00049.

[9] M.S. Anwer, B. Stieger, Sodium-dependent bile salt transporters of the SLC10A transporter family: more than solute transporters, Pflugers Arch. (2013) (Epub ahead of print).

[10] P.J. Meier, B. Stieger, Bile salt transporters, Annu. Rev. Physiol. 64 (2002) 635–661.

[11] C. Seeger, W.S. Mason, Sodium-dependent taurocholic cotransporting polypeptide: a candidate receptor for human hepatitis B virus, Gut 62 (2013) 1093–1095.

[12] R.B. Kim, B. Leake, M. Cvetkovic, M.M. Roden, J. Nadeau, A. Walubo, G.R. Wilkinson, Modulation by drugs of human hepatic sodium-dependent bile acid transporter (sodium taurocholate cotransporting polypeptide) activity, J. Pharmacol. Exp. Ther. 291 (1999) 1204–1209.

[13] S.K. Ladner, M.J. Otto, C.S. Barker, K. Zaifert, G.H. Wang, J.T. Guo, C. Seeger, R.W. King, Inducible expression of human hepatitis B virus (HBV) in stably transfected hepatoblastoma cells: a novel system for screening potential inhibitors of HBV replication, Antimicrob. Agents Chemother. 41 (1997) 1715–1720.

[14] K. Watashi, G. Liang, M. Iwamoto, H. Marusawa, N. Uchida, T. Daito, K. Kitamura, M. Muramatsu, H. Ohashi, T. Kiyohara, R. Suzuki, J. Li, S. Tong, Y. Tanaka, K. Murata, H. Aizaki, T. Wakita, Interleukin-1 and tumor necrosis factor-alpha trigger restriction of hepatitis B virus infection via a cytidine deaminase activation-induced cytidine deaminase (AID), J. Biol. Chem. 288 (2013) 31715–31727.

[15] S. Mita, H. Suzuki, H. Akita, H. Hayashi, R. Onuki, A.F. Hofmann, Y. Sugiyama, Inhibition of bile acid transport across Na+/taurocholate cotransporting polypeptide (SLC10A1) and bile salt export pump (ABCB 11)-coexpressing LLC-PK1 cells by cholestasis-inducing drugs, Drug Metab. Dispos. 34 (2006) 1575–1581.

[16] A. Schulze, K. Mills, T.S. Weiss, S. Urban, Hepatocyte polarization is essential for the productive entry of the hepatitis B virus, Hepatology 55 (2012) 373–383.

[17] M. Koyanagi, M. Hijikata, K. Watashi, O. Masui, K. Shimotohno, Centrosomal P4.1-associated protein is a new member of transcriptional coactivators for nuclear factor-kappaB, J. Biol. Chem. 280 (2005) 12430–12437.

[18] P. Gripon, I. Cannie, S. Urban, Efficient inhibition of hepatitis B virus infection by acylated peptides derived from the large viral surface protein, J. Virol. 79 (2005) 1613–1622.

[19] P. Gripon, C. Diot, A. Corlu, C. Guguen-Guillouzo, Regulation by dimethylsulfoxide, insulin, and corticosteroids of hepatitis B virus replication in a transfected human hepatoma cell line, J. Med. Virol. 28 (1989) 193–199.

[20] K. Watashi, A. Sluder, T. Daito, S. Matsunaga, A. Ryo, S. Nagamori, M. Iwamoto, S. Nakajima, S. Tsukuda, K. Borroto-Esoda, M. Sugiyama, Y. Tanaka, Y. Kanai, H. Kusuhara, M. Mizokami, T. Wakita, Cyclosporin A and its analogs inhibit hepatitis B virus entry into cultured hepatocytes through targeting a membrane transporter NTCP, Hepatology, in press.

[21] A. Schulze, P. Gripon, S. Urban, Hepatitis B virus infection initiates with a large surface protein-dependent binding to heparan sulfate proteoglycans, Hepatology 46 (2007) 1759–1768.

[22] O. Hantz, R. Parent, D. Durantel, P. Gripon, C. Guguen-Guillouzo, F. Zoulim, Persistence of the hepatitis B virus covalently closed circular DNA in HepaRG human hepatocyte-like cells, J. Gen. Virol. 90 (2009) 127–135.

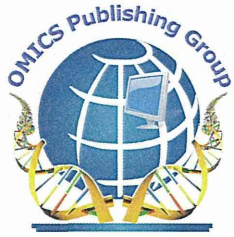


**ISSN: 2157-7439**

**Journal of Nanomedicine & Nanotechnology**

The International Open Access
Journal of Nanomedicine & Nanotechnology

## Special Issue Title:

### Nanotechnology: Challenges & Perspectives in Medicine

**Handling Editors**

**Malavosklish Bikram**
University of Houston, USA

**Available online at:** OMICS Publishing Group (www.omicsonline.org)



Digital Object Identi er: http://dx.doi.org/10.4172/2157-7439.S5-010

Nanomedicine & Nanotechnology

Gilmore et al., J Nanomed Nanotechol 2014, S5
http://dx.doi.org/10.4172/2157-7439.S5-010

Research Article Open Access

# Nanoimaging of ssRNA: Genome Architecture of the Hepatitis C Virus Revealed by Atomic Force Microscopy

**Jamie L Gilmore[1], Hideki Aizaki[2], Aiko Yoshida[1], Katashi Deguchi[1], Masahiro Kumeta[1], Julia Junghof[1], Takaji Wakita[2] and Kunio Takeyasu[1]***

[1]*Laboratory of Plasma Membrane and Nuclear Signaling, Kyoto University Graduate School of Biostudies, Yoshida-Konoe, Sakyo-ku, Kyoto 606-8501, Japan*
[2]*Virus Division II, National Institute of Infectious Diseases, Toyama, Shinjuku-ku, Tokyo 162-8640, Japan*

## Abstract

The complex structures that RNA molecules fold into play important roles in their ability to perform various functions in the cell. The structure and composition of viral RNA influences the ability of the virus to implement the various stages of the viral lifecycle and can influence the severity of the virus effects on the host. Although many individual secondary structures and some tertiary interactions of the Hepatitis C virus genome have previously been identified, the global 3D architecture of the full 9.6 kb genome still remains uncertain. One promising technique for the determination of the overall 3D structure of large RNA molecules is nanoimaging with Atomic Force Microscopy. In order to get an idea of the structure of the HCV genome, we imaged the RNA prepared in the presence of $Mg^{2+}$, which allowed us to observe the compact folded tertiary structure of the viral genome. In addition, to identify individual structural elements of the genome, we imaged the RNA prepared in the absence of $Mg^{2+}$, which allowed us to visualize the unfolded secondary structure of the genome. We were able to identify a recurring single stranded region of the genome in many of the RNA molecules which was about 58 nm long. This method opens up a whole new avenue for the study of the secondary and tertiary structure of long RNA molecules. This ability to ascertain RNA structure can aid in drawing associations between the structure and the function of the RNA in cells which is vital to the development of potential antiviral therapies.

**Keywords:** Hepatitis C Virus; Atomic Force Microscopy; Untranslated region

**Abbreviations:** HCV: Hepatitis C Virus; AFM: Atomic Force Microscopy; UTR: Untranslated Region

## Introduction

HCV is a worldwide epidemic, with about 150 million people worldwide infected and 350,000 deaths per year [1]. There is no vaccine for hepatitis C and treatments have met with limited success [2]. Given how pervasive HCV is, a better understanding of the virus may lead to important new discoveries which can help to highlight new avenues by which to treat individuals infected with the virus. Since HCV was originally cloned in 1989 [3], numerous studies have tried to understand the structure of the viral RNA, mainly in the conserved untranslated regions (UTRs) of the genome. Structural motifs that have been identified include the internal ribosome entry site (IRES) located in the 5'-UTR [4-17], the poly-U/UC region and 3'X RNA regions located in the 3'-UTR [18-24], and some stem loops in the coding region [25-29]. Additionally many long-range contacts between various regions of the genome have been reported [21,30-35]. Despite the vast number of reports on various structural features of the HCV genome, the full 3D architecture of the full genome remains uncertain.

Most techniques generally study bits and pieces of a single stranded (ss)RNA genome and hope to eventually arrive at the final global genome structure over time, or they provide data about various interactions within the molecule without providing 3D information [36]. The ability of Atomic Force Microscopy (AFM) to directly visualize the nanostructure of the whole genome in a variety of configurations in a single experiment makes it a very useful technique to assess the folded structures formed by a variety of ssRNA molecules. The usefulness of AFM for evaluating the nanometer scale architecture of biological molecules [37] was realized soon after the inception of the technology [38]. AFM has been used extensively for imaging of DNA with applications ranging from the study of DNA dynamics [39], DNA-protein interactions [40-45], to DNA origami structures [46,47]. However, techniques for obtaining reproducible ssRNA images have been slower to develop, leading to far fewer AFM imaging studies on ssRNA, although the nanometer scale resolution of AFM makes it a valuable tool for revealing the organization of ssRNA structures. Most AFM studies which have visualized ssRNA have used $Mg^{2+}$ concentration of 4-10 mM [48-52]. However, a couple of early studies [53,54], as well as a couple others studies of viral RNA [55,56] have achieved more extended ssRNA configurations using low salt solutions. It is well documented that ions play a much larger role in the folding of RNA tertiary structures, but play a minimal role in the formation of secondary structures formed by Watson-Crick base pairing of the nucleotides in the RNA chain [57-59]. Thus, by imaging various ssRNA molecules prepared without the addition of $Mg^{2+}$ ions, we should be able to get valuable information about the individual secondary structural motifs in the genome and and connectivity of the molecule.

In this study, we developed a method to observe both the secondary and tertiary structure of the full 9678 nt HCV genome with nanometer resolution using AFM. By omitting $Mg^{2+}$ from the buffer used to dilute the RNA prior to AFM imaging, we were able to observe the secondary structure of the molecule. The molecules had a linear configuration with various appendages extending from the molecule. Some commonly

***Corresponding author:** Kunio Takeyasu, Laboratory of Plasma Membrane and Nuclear Signaling, Kyoto University Graduate School of Biostudies, Sakyo-ku Yoshida-Konoe, Kyoto 606-8501, Japan, Tel/Fax: +81-75-753-6852; E-mail: takeyasu@lif.kyoto-u.ac.jp

**Received** January 27, 2014; **Accepted** February 22, 2014; **Published** February 24, 2014

**Citation:** Gilmore JL, Aizaki H, Yoshida A, Deguchi K, Kumeta M, et al. (2014) Nanoimaging of ssRNA: Genome Architecture of the Hepatitis C Virus Revealed by Atomic Force Microscopy. J Nanomed Nanotechol S5: 010. doi:10.4172/2157-7439.S5-010